Fellenius, B.H., 2019. Observations and analysis of wide piled foundations. Canadian Geotechnical Journal, 56(3), 378-397.

NRC
Research Press

Observations and analysis of wide piled foundations

Bengt H. Fellenius

Abstract: Available case histories on observations on full-scale piled rafts show that the settlement response to applied load can be modeled as that for an Equivalent Pier due to compression of the piles and the soil matrix plus that of an Equivalent Raft for compression of soil layers below the pile toe level. Interior piles engage the soil from the pile toe level upward in contrast to a single pile, which engages it from the ground downward. Piles and soil, combined as a pier, have strain compatibility, which determines the distribution of load between the piles, the contact stress, and the load-transfer movement of the piles. The responses between the interior and perimeter piles differ. Particularly so in non-subsiding and subsiding environment, because perimeter piles can be subjected to downdrag and drag forces, while neither downdrag nor drag force will affect the interior piles. In non-subsiding environment, it is advantageous to make perimeter piles shorter, while in subsiding environment perimeter piles best be longer. The load distribution across the raft is also governed by the degree of rigidity of the raft and by the difference in dishing at the pile toe level and in the dishing of the actual raft.

Key words: piles, pile groups, piles raft, settlement, load distribution.

Résumé : Les études de cas disponibles sur les radeaux empilés à grande échelle montrent que la réponse à la charge appliquée peut être modélisée comme celle d'un pieu équivalent dû à la compression des pieux et de la matrice du sol plus celle d'un radeau équivalent pour la compression des couches de sol du niveau de la pointe du pieu. Les pieux intérieurs amènent le sol du niveau de la pointe du pieu vers le haut contrairement à un seul pieu, qui l'engage du sol vers le bas. Les pieux et le sol, combinés comme un pieu, ont une compatibilité avec les contraintes, ce qui détermine la répartition de la charge entre les pieux, la contrainte de contact et le mouvement de transfert de charge des pieux. La réponse entre les pieux intérieurs et les pieux périmétriques diffèrent. Particulièrement dans les environnements sans affaissement et subsidence, parce que les pieux périphériques peuvent être soumis à des forces de traînée et de traînée, tandis que ni l'inclinaison descendante ni la force de traînée n'affecteront les pieux intérieurs. Dans un environnement non affaissant, il est avantageux de raccourcir les pieux périmétriques, tandis que dans les environnements de subsidence, les pieux périmétriques sont plus longs. La distribution de la charge à travers le radeau est également régie par le degré de rigidité du radeau et par la différence de cambrure au niveau de la pointe du pieu et au dégagement du radeau proprement dit. [Traduit par la Rédaction]

Mots-clés : pieux, groupes de pieux, radeau de pieu, règlement, répartition de la charge.

1. Introduction

The response of a single pile or narrow piled foundation to an applied load is well researched and fairly simple. The response of a wide piled foundation is a good deal more complex, however. Sometimes, the usually larger settlement response of a piled foundation, as opposed to that of a single pile supporting the same load as the average pile in the group, is taken as equal to the accumulated movements from each single-pile load–movement response of the piles in the group. This is a fallacious approach that has led to the development of many more or less complex methods for calculating settlement of a piled foundation, none correct (Fellenius 2016). When analyzing foundations based on a capacity reasoning, it is common to use a group capacity as the capacity of an equal number of single piles downgraded by an efficiency coefficient smaller than unity. This approach is also incorrect. It is a consequence of the fact that a pile group will impart stress to the soil below the pile toe level — the wider the group, the deeper the effect of the pile loads — and cause settlement to develop below the pile-toe level of the group interpreted as the average "capacity" of a pile in the group would be smaller than that of a single pile.

Sophisticated analysis methods exist that are based on correlating the response of a raft without piles, acting like a footing, to a pile-supported raft with the same total load. The contact stress under the footing part of the raft is thought to contribute to the accumulated "capacity" of the piles. In the most simplistic approach, the bearing capacity calculated for the footing without piles is added to the bearing capacity calculated for the pile. In some sophisticated approaches, the portions of load directed to the piles and to the footing, whether at sustained or ultimate conditions, are determined according to some correlation between the bending stiffness of the raft and the axial stiffness of the piles.

In engineering practice, the analysis of piles and piled foundations is dominantly based on an ultimate resistance approach, requiring the factored supported load to be a fraction of the ultimate resistance as determined by a resistance factor. No allowance is given to any bearing resistance of the pile cap (pile raft). Because buildings and other structures are these days heavier than in the past and the conventional analysis approach results in expensive foundations, it has become increasingly common to include a contribution to the bearing from the pile cap or pile raft (the concept is actually the other way around, the piles are considered to contribute to the bearing of the raft). Such foundations

Table 1. Details of reviewed case histories.

Case	Diameter (mm)	Depth (m)	Spacing (× b)	Footprint ratio (%)	Soil type	Settlement	Distribution	Contact stress
2.1	500	6	3	10	Soft clay	X	—	—
2.2	600	9	4	8	Fines	X	—	—
2.3	1000	42	4	8	Fines	X	—	—
2.4	520	13	4	5	Fines	X	—	—
2.5	460	22	5	4	Fines	X	—	—
2.6	1800	30	3	12	Fines	X	—	—
2.7	300	26	7	2	Soft clay	X	X	X
2.7	300	28	11	0.8	Soft clay	X	X	X
2.8	406	48	3	9	Fines	X	X	X
2.9	300	48	10	0.9	Fines	—	—	X
2.10	600–1200	46	10	0.9	Fines	X	X	X
2.11	900–1200	45	—	—	Fines	X	X	X
2.12	400	24	11	0.5	Fines	X	—	X
2.13	700	40	2	18	Fines	—	X	—
2.14	350	24–36	—	4.8	Soft clay	X	X	—

Note: *b* = pile diameter.

are often called "pile-enhanced footings" or "piled-raft foundations". The combined bearing is attributed to the combined ultimate resistance of piles and bearing capacity of the raft. The analysis then applies the condition that the working load is governed by a factor of safety (or resistance factor) applied to the combined ultimate resistance of the piles and raft. The fallacy here is the bearing capacity concept; that is, correlating the response to an artificially increased load — the "capacity". Instead, the relevant response of the foundation is in regard to the working load and it must be addressed in terms of foundation settlement.

There is an overall dearth of case histories that report measurements of "wide" groups. Wide piled rafts can be defined as having pile groups wider than four pile rows, i.e., minimum 25 piles, in total. Most available case histories on full-scale pile groups, few as they are, are limited to reporting settlement of the pile raft, only, and, usually, only report the pile head movement for an applied load; as in a hydro test, a short-term condition. Only a couple of case histories exist that show measurement of axial load in the piles with depth and contact stress between the pile cap and soil. I know no publication reporting soil stress with depth in-between the piles. Available records of wide piled foundations' response to load are cited in the following. Table 1 compiles details of the case histories.

2. Case histories

2.1. Broms (1976)

Broms (1976) reported settlement measured for two rectangular embankments on a 15 m thick deposit of compressible soft clay. One of the two embankments was supported on a grid of 500 mm diameter, 6 m deep lime-columns ("soft piles") placed at a center-to-center spacing of 1.4 m (2.8 × column-diameter). The Footprint Ratio, i.e., ratio between total column ("pile") area and total footprint area, was about 10%.

Figure 1 combines the measurements from the two embankments taken at 16, 65, 351, and 541 days after constructing the embankment. "Column Area" indicates records under the embankment supported on 6 m long lime-columns and "Reference Area" indicates an adjacent embankment with no columns. The measurements showed that the settlement for the column-supported embankment was not only smaller, but also more uniform than under the no-column reference area.

Although the axial stiffness of the lime column is many times smaller than that of a similar size concrete pile, it is still many times larger than that of the soft clay, and, if freed (excavated), it appears similar to a pile. It is, therefore, rational to draw a parallel between the embankment supported on the lime columns and an embankment, or flexible raft, supported on piles — the difference

Fig. 1. Settlement of lime-column supported and unsupported embankments on soft compressible clay (data from Broms 1976).
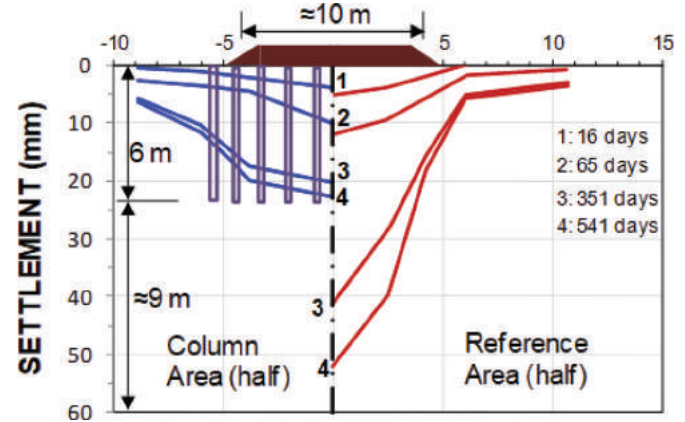
is more in terminology than in mode of behavior. A suitable model for analyzing the two embankments is to calculate the settlement of the Reference Area as that of a flexible raft placed at the ground surface. The settlement of the Column Area is calculated as that of an Equivalent Pier within the column depth combined with a flexible Equivalent Raft at the column depth. Boussinesq stress distribution is applied to both models. The calculated settlement is the sum of the consolidation settlement for the Equivalent Raft and the compression of the lime-column-reinforced upper 6 m of clay.

The settlements were calculated using the UniSettle software (Goudreault and Fellenius 2011) and matched to the settlement measured at the center of the embankment. (The UniSettle software applies conventional settlement theory comprising immediate compression, consolidation settlement, secondary compression, and effective stress distribution, for input of soil densities, preconsolidation stresses, OCR, preconsolidation margins, virgin and reloading compressibilities, coefficients of consolidation, and secondary compression coefficients). The same parameters for the soil below 6 m depth were used under the Column Area as for the Reference Area. On shifting the calculation to the other measuring points, the points within and outside of the footprint, no changes were made other than those entailed by the Boussinesq distribution. The calculation results were found to also match those observations without any further input.

Broms (1976) stated that the settlements measured outside the column area indicated that the column-reinforced pier (or block)

**Fig. 2.** Settlement vs. time in linear and logarithmic time scales (data from Golder and Osler 1968).
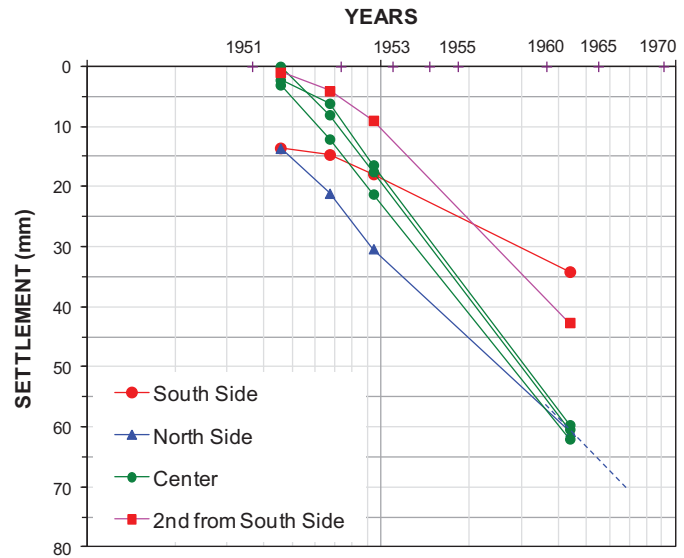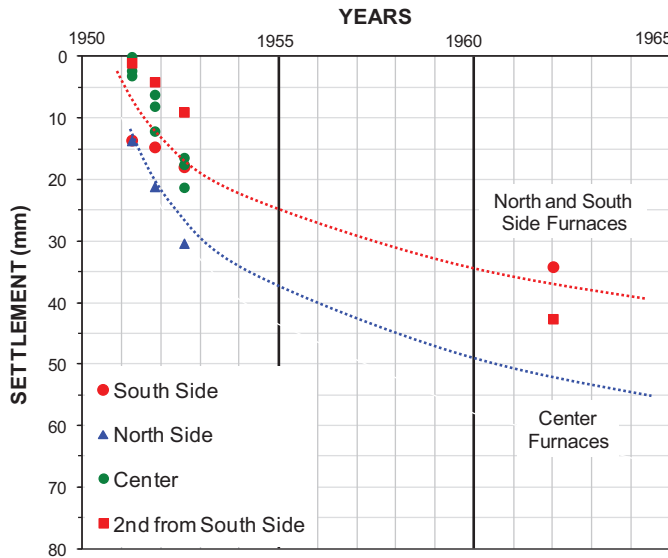
transferred load through shaft resistance acting along its enveloping perimeter that imposed consolidation in the surrounding clay. However, as the calculations using the UniSettle software show, the settlement measured outside the footprint area is more likely caused by the stress from the embankment load acting at the toe of the lime columns or at the ground surface of the reference embankment.

2.2. Golder and Osler (1968)

Golder and Osler (1968) presented 12 years of settlement measurements of a bank of five furnaces placed with long sides in parallel next to each other at a depth of 1.5 m and about 6 m apart over a total footprint of about 16 m by 54 m. Each furnace had a 16 m by 10 m footprint and was supported on a group of thirty-two, 600 mm diameter expanded-base piles (Franki piles) installed to a depth of 8.5 m and at center-to-center spacing ranging from 2.1 m to 3.2 m. The average Footprint Ratio (total cross sectional area of the piles over total foundation footprint) was about 6%. The total furnace load was 21 MN/unit, that is, 670 kN per pile and an average stress of 130 kPa over each furnace footprint. The soil profile consisted of an upper 24 m thick, compact to dense sand deposit on a more than 50 m thick layer of soft compressible clay. The groundwater table was at 4 m depth. A static loading test to 1800 kN, performed before constructing the furnaces, showed a 3 mm maximum pile head movement.

The furnaces were built in early 1951. Settlement of the furnaces was monitored until January 1962 at six benchmarks placed between the furnaces. Figure 2 shows the settlements over time for the furnaces from April 1951 (when all five furnaces were completed) through January 1962 for time in both linear and logarithmic scales. The straight-line development of the settlements vs. log of time diagram implies that consolidation settlement was continuing when the last (1962) readings were taken.

Figure 3 shows the settlement measured along the center of the furnaces and the settlement calculated using Boussinesq stress distribution, compressibility parameters, settlement, and conventional consolidation approach, as fitted to the January 1962 settlement for the center of Furnace 3. The parameters obtained by the fitting were used to calculate the settlements for a flexible Equivalent Raft placed at the pile toe level. As indicated in the figure, the calculated and measured values outside the fitted point agree well.

It is obvious that the measured settlement is entirely from consolidation of the thick soft compressible clay below the sand layer.

Fig. 3. Measured and calculated settlements along center of the furnaces (data from Golder and Osler 1968).
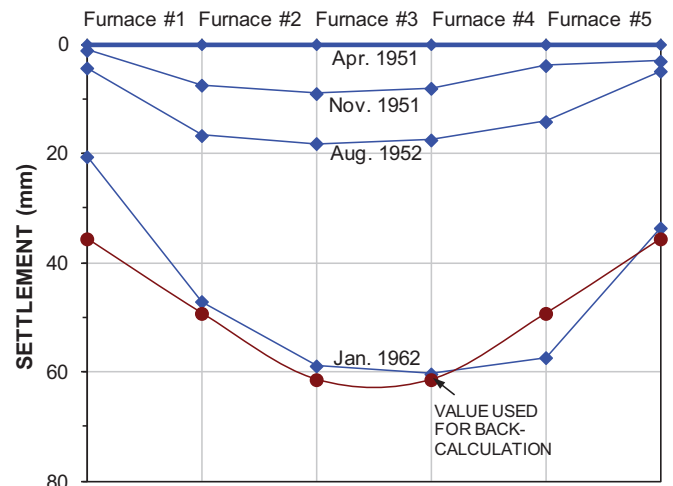
2.3. Badellas et al. (1988)

Badellas et al. (1988) presented a case history of settlement measurements for a 38 m diameter, liquid storage tank in Thessaloniki, Greece, supported on a piled foundation comprising 112 piles (also discussed by Georgiadis et al. 1989 and Savvaidis 2003). The soil profile consisted of 40 m of soft compressible soil followed by dense silty sand. The groundwater table was at about 1.5 m depth.

The tank bottom consisted of an 800 mm thick concrete raft and the total dead weight of the empty tank was 70 MN (about 60 kPa stress). The piles were bored piles, 1000 mm in diameter and 42 m in length (i.e., seated about 2 m into the dense sand). The Footprint Ratio was about 8% and the average spacing was about 3.6 pile diameters. Figure 4 shows the layout of the piles. The locations of three piles, Piles 7, 11, and 16, monitored for settlement during a hydrotest, are indicated in the figure.

A 30-day hydrotest to a height of about 17 m was performed with 10 days of loading, 10 days of holding the height, and 10 days of removing the water. Figure 5A shows the sequence of water loading and the measured settlements. Figure 5B shows the settlements measured during the hydrotest for the three monitored piles.

Fig. 4. Layout of the piles for the Thessaloniki tank (data from Badellas et al. 1988).
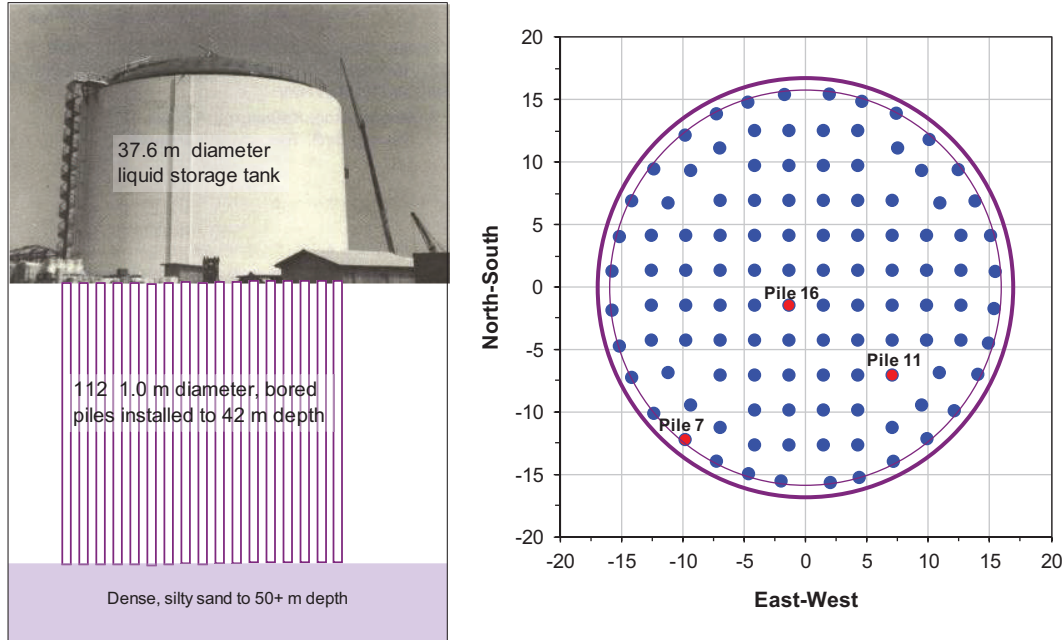

Fig. 5. Hydrotest for the Thessaloniki tank showing (*A*) water height in tank and (*B*) settlements measured at three piles (data from Savvaidis 2003).
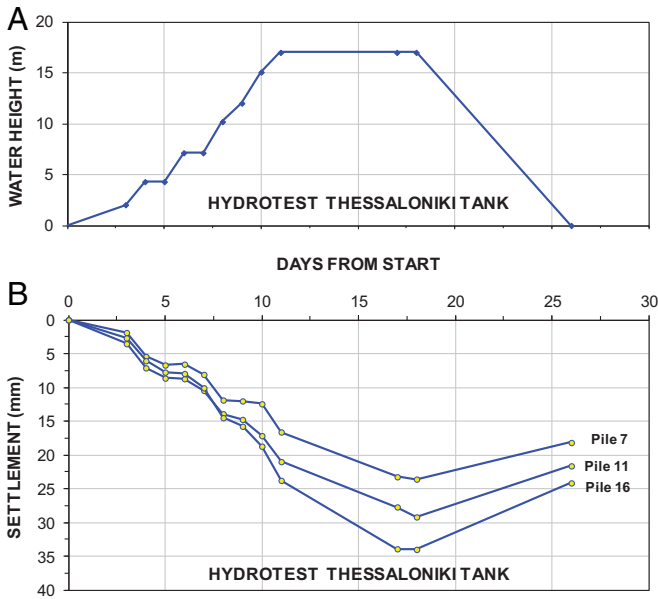

Fig. 6. Measured and calculated settlements for the Thessaloniki hydro tested tank along the tank diameter (data from Badellas et al. 1988).

Conventional soil compressibility parameters obtained from the best-fit between measured and calculated settlements for the preloading event gave settlement values for the hydrotest event that were in a good agreement between measured and calculated settlements of the tank center and perimeter.

Figure 6 shows the settlement measured along a diameter of the tank settlement just before unloading the tank, as extracted from a contour line graph in the original paper. The extracted distribution also indicates that the piled foundation responded to the loading and settlement as a flexible raft. I have back-calculated the settlement for an Equivalent Raft placed at the pile toe depth with the load-spreading to the raft per the mentioned method, using the fitted conditions to calculate the settlement along the

full diameter. The calculations assumed negligible compression of the piles and that, in calculating the settlements, the pile group could be modeled as a raft loaded uniformly with the weight of the tank and its stored liquid. The resulting soil parameters indicated a 100 kPa preconsolidation margin ($\sigma'_p - \sigma'_0$), a 25 MPa virgin elastic modulus ($m = 250$), and a 50 MPa re-compression elastic modulus ($m_r = 500$). The stress below the raft was per Boussinesq distribution.

2.4. Goossens and van Impe (1991)

Goossens and van Impe (1991) presented results of 10 years of monitoring settlement along the side of a tightly spaced group of 40 grain silos, 52 m in height, founded on a 1.2 m thick concrete raft with an 84 m by 34 m footprint. The raft was supported on 697 piles, consisting of 520 mm diameter, 13.4 m long, driven, cast-in-place concrete piles with expanded base (Franki piles) with a working load of about 1200 kN. Two static loading tests to 2250 kN performed before constructing the furnaces showed a maximum pile head movement of 7 mm. The average Footprint Ratio was 5% and the pile spacing, c/c, was 4 pile diameters. The soil profile below the pile toe level consisted of sand alternating with compressible clay to 33 m depth. The groundwater table was at 3.0 m depth. For fully loaded silos, the total load distributed

Fig. 7. Measured and calculated settlements along the side of the silo foundation raft and calculated for center line (data from Goossens and van Impe 1991).
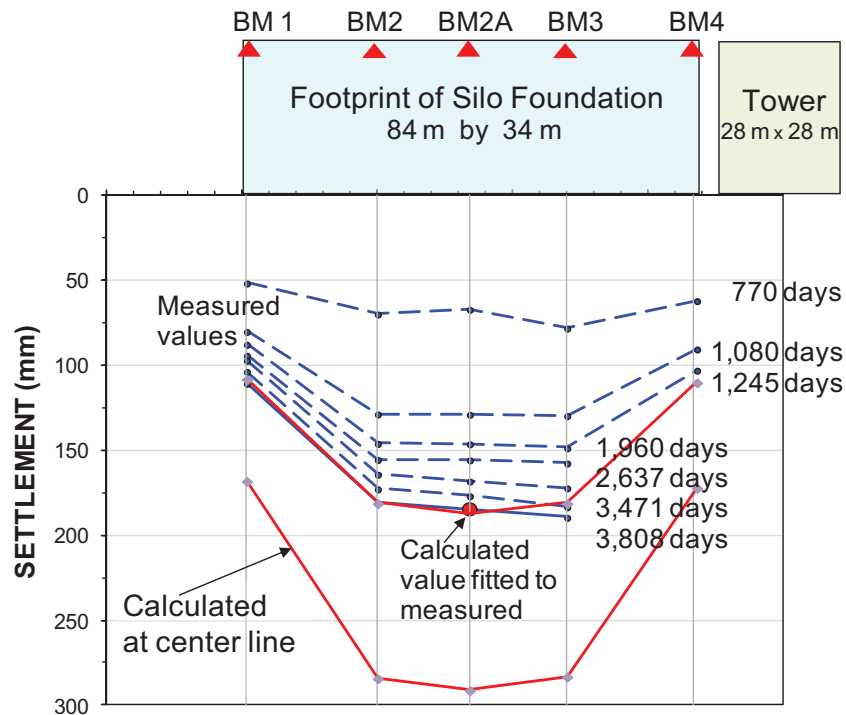
evenly across the footprint corresponded to a stress of about 300 kPa.

Based on the results of the static loading test, the settlement of the piled foundation was expected to be small. Still, to investigate the long-term development, a programme of settlement monitoring at five benchmarks affixed to the raft along one side was implemented. In Fig. 7, the upper solid line shows the settlement measured at the benchmarks. The dashed lines show the settlements for the benchmarks as back-calculated using Boussinesq stress distribution, compressibility parameters, and a conventional consolidation approach for a flexible raft placed at the pile toe level with input parameters to fit calculated settlement to measured settlement at the middle benchmark for Day 1245. The calculated values included an Equivalent Pier compression plus pile toe penetration smaller than 10 mm. The fit of calculated value to the measured value at Benchmark BM2A calibrated the input to the analysis.

Figure 7 also shows a settlement curve (solid line) back-calculated for the center line of the piled raft foundation using the so-calibrated soil parameters. The settlements calculated for the center line indicate that the differential settlement between the center and the corner would have been about 200 mm over 40 m, about 1:200. However, Goossens and van Impe (1991) reported no sign of distress for the silo structure.

Again, the good match between the settlement measured at the benchmarks and the values calculated using the parameters matched to the settlement at the BM2A benchmark indicates that the settlement of the piled foundation can be correctly modeled by a conventional analysis applied to an Equivalent Pier on an Equivalent Raft at the pile toe level with Boussinesq stress distribution.

2.5. van Impe et al. (2013)

van Impe et al. (2013) analyzed a case of settlements of three 33 000 m³ in volume, 19 m tall oil tanks, each supported on 422 piles (also discussed by Fellenius 2014; van Impe and Bottiau 2016; van Impe et al. 2018). The piles were 460 mm diameter,

21.6 m long screw piles (Omega piles). The soil profile consisted of a 15 m thick old fill of sand with clay deposited on about 4 m of silt and clay and 5 m of sand on a tertiary, slightly overconsolidated stiff clay at 24 m depth that continued for about 100 m.

Each pile cap was a 49 m wide and 600 mm thick reinforced concrete slab. The total load from the filled tanks was about 330 MN, giving an average maximum pile load of 780 kN and an about 200 kPa average stress over the tank footprint. The Footprint Ratio was 4% and the average center-to-center pile spacing was 2.2 m (about 5 pile diameters). The pile was very flexible, but, as the free length from pile to pile was short, the slab can be considered capable of bridging the 200 kPa stress with minimal bending of the raft.

Figure 8 shows the pile head, pile shaft, pile toe, and pile compression load–movement curves of a static loading test. The results indicate no obvious ultimate resistance. The pile capacity can be estimated to range from about 3100 kN at a pile head movement of 40 mm to about 3600 kN at about 70 mm movement. The settlement within the pile length will be small; as indicated by the measured pile compression, it would be only a millimetre or two. Therefore, settlement of the tanks will be governed by the compression of the tertiary clay underneath the sand "cushion" immediately below the pile toe level.

Hydro-testing of the three tanks was performed in April 2013, by filling one tank at a time with water to a height of about 18 m, which took about 6 days. The maximum water level in the tank was then maintained constant for about 4 days, whereafter the tanks were emptied over 3 days. The free distance between the tanks was 17 m, which is smaller than the 22 m depth to the pile-toe level. Tank 1 was filled and emptied first. Tank 2 was then filled. This meant that the water load in tank 1 was preloading the soil under Tanks 2 and 3; more under the side closest to Tank 1 than for the away side. Similarly, Tank 2 added preloading of the soil under Tank 3.

After the 4 days of maintaining the maximum water height in Tank 2, it was emptied by pumping the water over to fill Tank 3.

Fig. 8. Load movement curves for head, shaft, toe, and compression (data from Fellenius 2014).
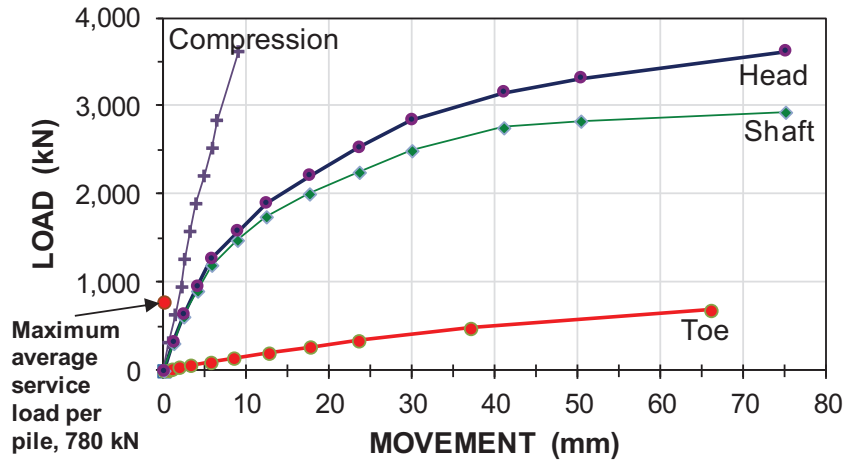

Fig. 9. Measured perimeter settlements for Tanks 1 and 2 at maximum load and remaining settlement of Tank 1 after unloading. North direction assumed vertical. (Data from van Impe et al. 2013).
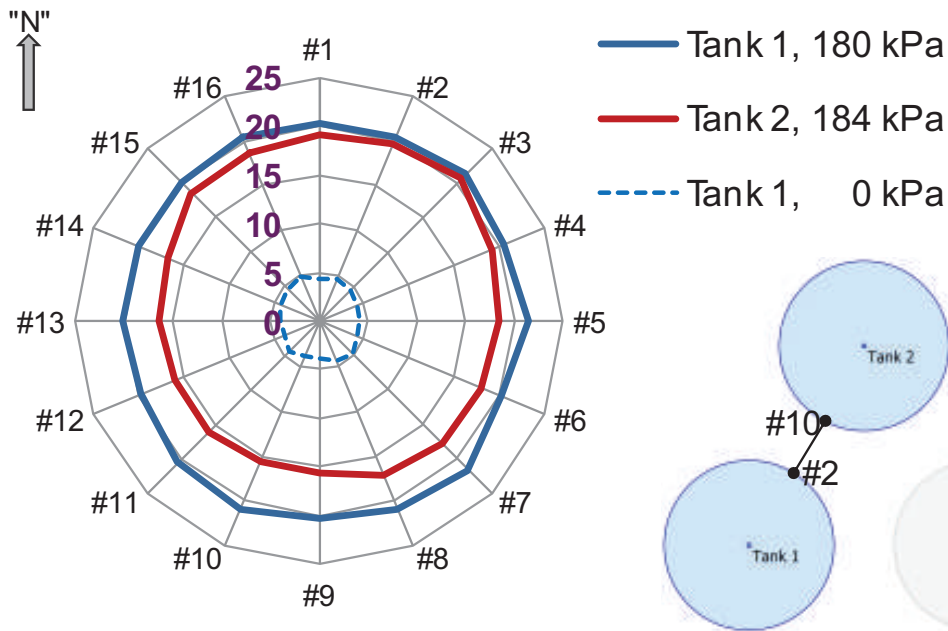
This procedure means that the filling of Tank 3 started when the stress from Tank 2 was present under Tank 3 and that this stress reduced at the same rate as the stress induced from the load in Tank 3 increased.

Figure 9 shows the observed settlements for Tanks 1 and 2 at maximum load and remaining settlement of Tank 1 after unloading. The settlement for the #2 gages (benchmarks) in Tanks 1 and 2 are about equal, while the settlement for #10 gages show larger settlement for Tank 1 than for Tank 2, possibly, because the preloading effect reduced the settlement under the Tank 2 side closest to Tank 1.

Figure 10 shows the observed perimeter settlements for all three tanks (settlement of Tank 3 added) at maximum load and the remaining settlement of Tank 3 after unloading. No preloading effect similar to that shown in Fig. 9 is noticeable.

Because of the variable condition and the interference between the pile groups, no advanced numerical analysis is practically possible that considers the pile loads and interaction between the piles. However, it is simple to model the case as three Equivalent Piers each with an Equivalent Raft at the pile toe level. I have fitted

a calculation using such a model adjusted to the measured settlement of the tank center. Repeating the calculation for the perimeter measuring points away from and close to neighboring tanks without adjustment to the soil parameters showed agreement between calculated and measured values (Fellenius 2014). The results show that the Equivalent Pier analysis and Boussinesq stress distribution with due consideration of the interactive stress distribution does satisfactorily model the measured settlement and interference between the pile groups.

2.6. Gwizdala and Kesik (2015)

Gwizdala and Kesik (2015) reported settlement records taken on the Third Millennium Bridge in Gdansk, Poland, a cable-stayed road bridge, constructed in 1999–2001, spanning the Dead Vistula River and linking up the Northern Port of Gdansk with the national road network. The main bridge component is a single tower, a 100 m tall reinforced concrete pylon, consisting of a 52.4 m × 22.4 m concrete slab supported on 50 bored piles of 1800 mm diameter and 30 m embedment. The total unfactored load was 480 MN and the unfactored working load per pile was

Fig. 10. Measured perimeter settlements for tanks 1, 2, and 3 at maximum load and remaining settlement of tank 3 after unloading. North direction is assumed vertical. (Data from van Impe et al. 2013).
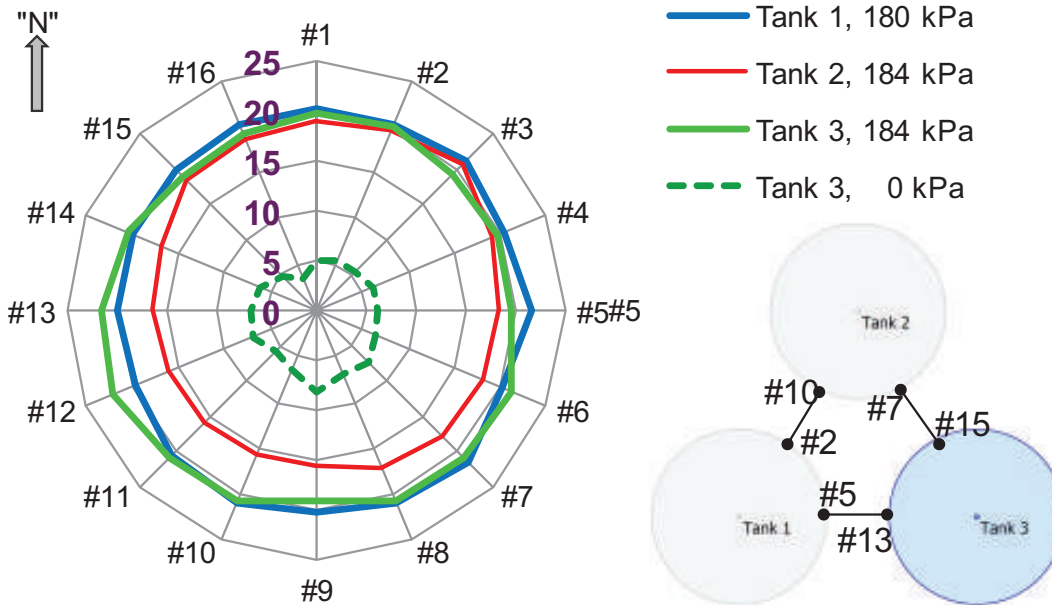
Fig. 11. Pylon pile layout for the Third Millennium Bridge, Gdansk (data from Gwizdala and Kesik 2015).
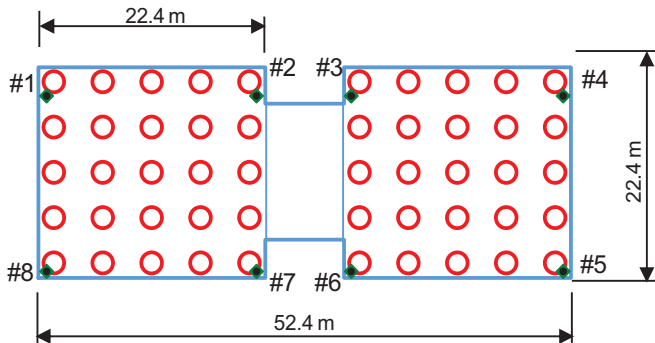
Fig. 12. Vertical section and geometry of the pier.

Fig. 13. Measured settlements (data from Gwizdala and Kesik 2015).
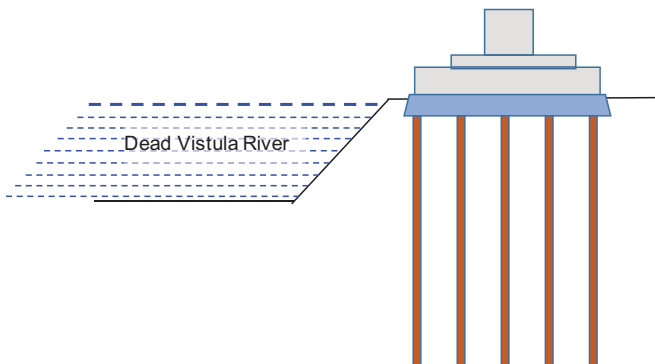
9600 kN. The soil profile consisted of 25 m of interbedded clay and sand deposited on sand.

As shown in Fig. 11, the piled foundation has the form of two square grids of 25 piles each with a 5.8 m, 3.3 diameter center-to-center spacing and an about 12% Footprint Ratio.

Figure 12 shows a vertical section of the foundation and the geometry toward the river. The foundation lies close to and parallel to the river. Starting after the casting of the slab, the pylon

settlement was monitored over time, at eight locations around the slab, Points #1 to #8 in Fig. 11. Figure 13 shows that the tower had a slight tilt, i.e., the measured settlements differed between the land side and the river side.

I have modelled the piled foundation as an Equivalent Pier on a flexible raft at the pile-toe level and calculated the settlement as compression of the piles for the axial load and from consolidation of the soil below the pile-toe level, using a compressibility input that gave a settlement matching the average (assumed to be that at the center of the foundation). The calculated settlements and the consolidation coefficient were matched to those measured at about 700 days (end of construction) and at about 1700 days (after the following about 1000 days of consolidation). The input geometry included modeling the river as an "excavation", which resulted in an "unloading" of the deeper soils. The "unloading" resulted in smaller settlement along the river side and larger settlement along the land side, which is also what the calculation results show using Boussinesq distribution. Thus, the calculation results, again, confirm that the assumption of Equivalent Raft in combination with conventional approach to effective stress dis-

Fig. 14. Plan of Building 2 and locations of test piles and earth stress cells (data from Hansbo 1984).
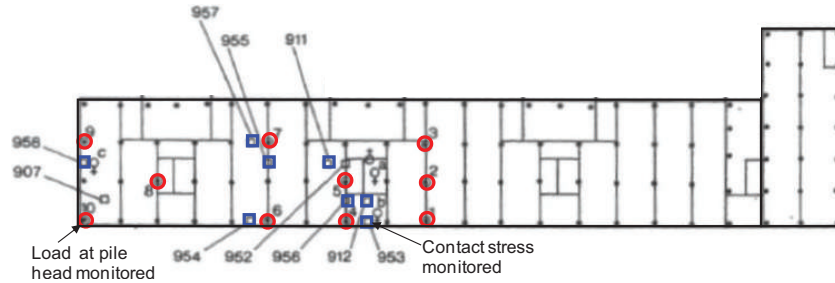
tribution is a suitable model of the settlement of the piled foundation.

Gwizdala and Kesik (2015) applied the Polish code to their analysis, which includes an Equivalent Pier approach where the bottom raft is wider than the actual raft at the foundation level. The widening starts at the pile head. In back-calculating the average settlement of the two rafts, the authors also applied an E-modulus taken from the geotechnical investigation and assumed that it increased with depth. The main difference between my analysis and the authors' is my recognition and inclusion of the "unloading" effect of the river.

2.7. Hansbo (1984, 1993) and Hansbo and Jendeby (1998)

Hansbo (1984, 1993) and Hansbo and Jendeby (1998) monitored the long-term response of two adjacent four-storey buildings (Buildings 1 and 2) in Göteborg, Sweden, that were supported on 18 m long wood piles in soft clay equipped with an upper 10 and 8 m extension, respectively, of a 270 and 300 mm diameter square precast concrete pile, respectively. The Building 1 foundation was a grillage of beams (contact area was not reported) and Building 2 was a piled raft. The footprints were 50 m × 14 m and 75 m × 12 m, respectively.

The soil profile consisted of soft to very soft, compressible, normally consolidated, marine clay extending to about 40 m depth. The general area is subject to a small general subsidence, about a millimetre or two per year. The nominal total loads on the foundations of the two buildings were 46 and 54 MN, respectively, corresponding to an average stress over the building footprint of 66 and 60 kPa, respectively, which are very similar values. The number of piles was 211 and 104, respectively, corresponding to average axial working loads of 220 and 520 kN/pile, respectively, if applied only to the piles. A conservatively estimated pile "capacity" was 330 kN.

The average plan areas per pile were 3.3 and 8.7 m², the pile c/c distances were about 7 and 11 pile diameters, and the Footprint Ratios were 2.0% and 0.8%, respectively. Building 1 was placed on a rigid ground-beam grillage. The total contact area of the beam grillage was not reported. Building 2 was placed on a 500 mm thick raft. Prior to construction, soil was removed to about 3 m depth across the building footprint areas.

Both foundations were instrumented with load cells to monitor the load at the head of a few piles (flat jacks) and contact stress (earth stress cells) under the beams and raft, respectively. Figure 14 shows the layout of Building 2 with locations of piles for load measurements and stress cells.

Observations over a 13 year period showed that Buildings 1 and 2 settled about the same amount: 44 and 41 mm, respectively. That is, the settlements correspond to the average stress rather than to load per pile. Figure 15 shows the average settlements measured during 13 years. I have plotted the settlement records in relation to the settlement (41 mm) measured last (1993). The largest settlement, 50 mm, in building 1 occurred at a benchmark placed in the center portion of the building footprint and the smallest, 36 mm, along the perimeter and corners. For building 2, the settlement in the center ranged from 42 to 48 mm and the settlement along the

Fig. 15. Average building settlement measured during 13 years (data from Hansbo and Jendeby 1998).
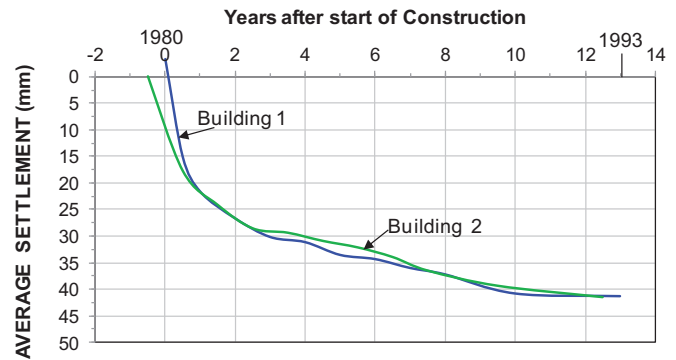
perimeter and at corners ranged from 32 to 40 mm. Measurements of settlement with depth near perimeter piles indicated that about 75% of the settlement and relative movement between the piles and the soil developed below about 18 and 14 m above the pile toe level, respectively. Settlements below the pile toe level were small.

At the end of construction, the measured average pile loads in the center of the buildings were about 150 and 300 kN for Buildings 1 and 2, respectively. The average stress due to these loads as distributed over the each building footprint was 45 and 35 kPa, respectively, corresponding to 70% and 60%, respectively, of the total nominal loads for the buildings. The contact stress measured for Building 2 in three cells along the perimeter of the building ranged from 25 to 50 kPa.

Hansbo and Jendeby (1998) reported that the Building 1 average pile load reduced with time, but did not separate the observations on perimeter piles and interior piles. The axial load in the piles will have increased due to accumulation of negative skin friction from the regional subsidence (build-up of drag force), the load applied to the perimeter piles from the ground slab will have decreased (the pile response will have softened). As a consequence, the interior piles (only 10 piles were monitored) will have experienced an increase of load. The process is similar to that reported by Russo and Viggiani (1995), see below.

The data show that the Equivalent Pier E-modulus for Building 1 was about twice that of Building 2. Thus, the calculated compression of Building 1 was about 10 mm while the calculated compression of Building 2 was about 20 mm, leaving about 30 and 20 mm, respectively, of the settlement to have been due to load transfer and settlement underneath the pile toe level. However, the settlement monitoring indicated that the settlement below the pile toe level was a small part of these values as opposed to about equal. Moreover, that the load transfer would be larger from the foundation with the larger number of piles and smaller pile loads is counterintuitive, however, and puts some constraint on the detailed analysis.

Fig. 16. Pile layout at the main pier of the Garigliano bridge (after Russo and Viggiani 1995; Mandolini et al. 2005).
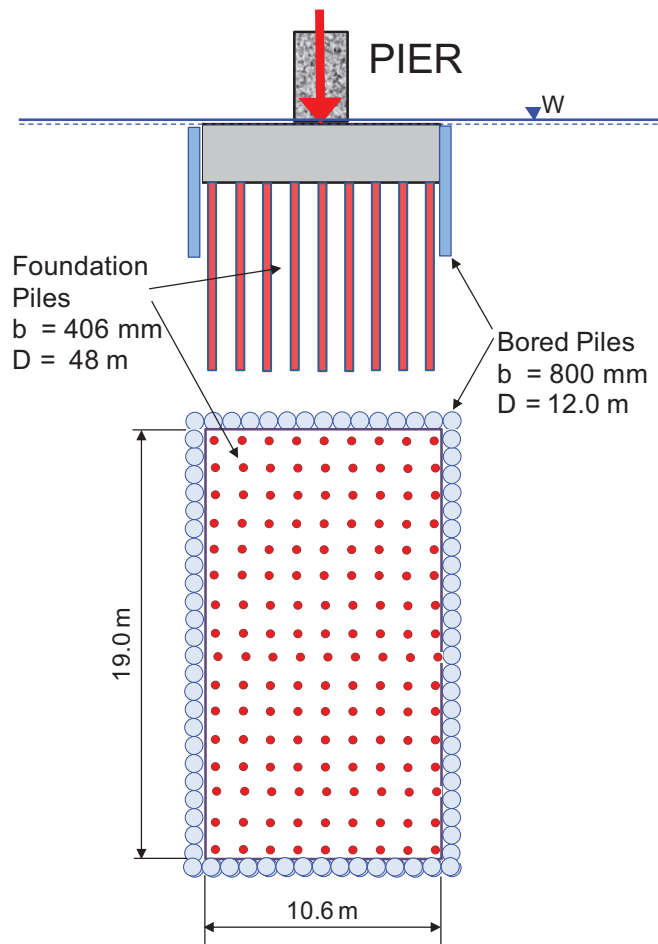
2.8. Russo and Viggiani (1995) and Mandolini et al. (2005)

Russo and Viggiani (1995) and Mandolini et al. (2005) reported a case history of a piled foundation of the main pier of a cable-stayed bridge over the Garigliano River in Southern Italy; constructed in 1991–94. The soil profile consisted of about 10 m of clay on about 10 m of dense sand underlain by soft clay deposited at about 48 m depth on a very dense sand and gravel bed. The clay is normally consolidated undergoing small regional subsidence.

The piled foundation comprised 144 mandrel-driven, then concrete-filled, steel pipe piles, 406 mm diameter, 48 m long, uniformly distributed in a 10.6 m by 19.0 m raft (Russo and Viggiani 1995), as shown in Fig. 16. The piles were driven into the very dense sand and gravel layer. The pile configuration was rectangular, comprising 9 rows and 16 columns, and the pile c/c distance was 1.2 m (3.0 pile diameters). The Footprint Ratio was 9%. Enveloping the raft, a wall of 800 mm diameter bored piles to 12 m depth was constructed to protect against scour. These piles were free from contact with the raft and the pipe piles. The unfactored load from the pier was 800 kN/pile, which incorporated a factor of safety of 3.0 on pile capacity as stated to have been verified in static loading tests.

The foundation was instrumented to monitor the pile axial load in 35 piles and the contact stress between the raft and the soil in eight earth-stress cells, as the bridge was constructed. The measurements showed that after the construction of the bridge had been completed, interior piles under the raft carried 60% of the load carried by corner piles.

Figure 17 shows the approximate development with time of measured axial loads in interior, side, and corner piles. After the

bridge had been constructed, two trends in the distribution of pile loads can be seen: the load on the interior piles increased and the load on the corner and side (edge) piles decreased, while the total load on the piles increased by 10% (Mandolini et al. 2005). The authors suggested that the observed trend of increase of load on the center piles and decrease of load on the corner and perimeter piles was due to creep of the reinforced concrete raft. However, I believe that the trends were more likely because the regional subsidence developed negative skin friction along the perimeter piles causing their response to the raft load to become less stiff. Moreover, the accumulated negative skin friction (i.e., drag force) added to the total load on the raft. The interior piles were shielded from the effect of downdrag due to negative skin friction. Had the 12 m long scour-protecting piles not been providing additional shielding, the observed re-distribution of load and increase of toe resistance would likely have been more pronounced. Moreover, due to the fact that the response of the more slender and shorter 12 m piles bearing in sand, as opposed to the 48 m piles, was considerably softer than the 48 m piles, it is logical that their axial load was low, resulting in the 48 m piles supporting the silos with no appreciable contribution from the 12 m piles.

The authors reported that the stress at the raft–soil interface (contact stress) measured in the eight pressure cells was almost negligible at all stages. However, the actual stress values were not reported.

## 2.9. Auxilia et al. (2009)

Auxilia et al. (2009) presented measurements of raft–soil interface (contact stress) for three 70 m tall cement silos founded in a soil profile consisting of about 25 m of compact sand on 17 m of soft to firm silt and clay to 43 m depth followed by dense gravel and gravelly sand. The piled foundation consisted of 110 driven cast-in-situ piles of 400 mm diameter, 12 m long intended as soil-reinforcement and 19 bored piles, 1500 mm diameter, 48 m long terminating in the dense gravel and gravelly sand. The bored piles were distributed underneath the silo walls. The Footprint Ratio was 0.9%, which corresponds to an average pile spacing of 10 diameters. The raft was 40 m wide and 1.8 m thick. When the raft had been cast on the piles and ground, the contact stress measured in the dredged silty sand fill underneath the raft registered 15 kPa, which value then remained as the silos were constructed. At a 194 MN total load, composed of silo self-weight and about 35% of the final silo load, the load in the 110, 12 m long interior piles was 100 kN/pile, corresponding to a strain of about 25 $\mu\varepsilon$. The total load at the head of interior piles was 60% the total load at perimeter piles. The 15 kPa contact stress together with a strain equal to the 25 $\mu\varepsilon$ in the piles indicates an E-modulus of approximately 1 MPa, which suggests a rather loose condition of the silty sand.

2.10. Yamashita et al. (2013)

Yamashita et al. (2013) reported observations of a 56 m tall building on a continuous 100 m by 120 m footprint area, 600 mm thick raft during construction and during 1 year afterward. The soil profile consisted of 44 m of soft silt and clay followed by dense sand. The raft foundations consisted of 600 and 1200 mm diameter bored piles constructed into the top of the sand, at a spacing of about 10 to 12 pile diameters. The foundation also included a ground improvement system of 1 m wide cement–soil walls to 20 m depth below the original ground surface (13 and 16 m below underside of the foundation raft). The cement–soil walls were placed in a 9.6 m wide square grid. The piles were slightly off-center in that grid.

The observations comprised measurements of pile head loads of four piles, one of which also had gages to measure the axial load at 30 and 35 m depth. To measure contact stress, total stress cells were placed on the excavated and prepared ground underneath

Fig. 17. Measured axial load during and after construction (data from Russo and Viggiani 1995).
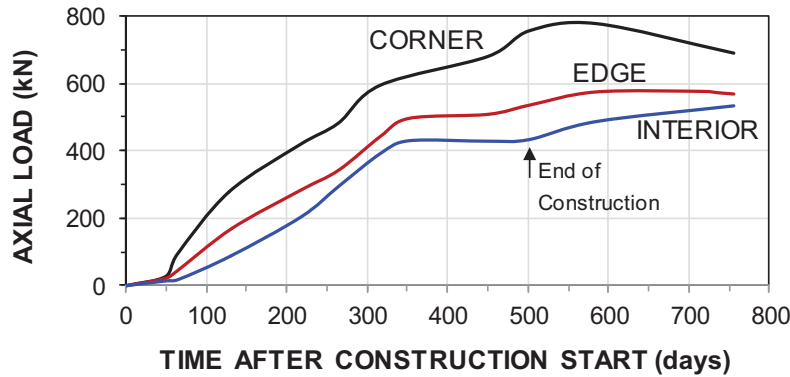
the raft. Three cells were placed over the area of natural soil and three were placed on the cement–soil walls. One piezometer was also installed below the raft to enable establishing of the effective contact stress. One year after the end of construction, the load supported by the 1.2 m diameter bored pile was 10.8 MN. Combining the 10.8 MN pile load with the 1.15 m^2 pile area and an assumed E-modulus of 25 GPa for the concrete pile gives a pile strain of about 400 $\mu\varepsilon$. Strain compatibility requires that the soil underneath the raft experience the same 400 $\mu\varepsilon$.

At the end of construction, the measured contact stresses were 114 kPa at the cement–soil wall and 28 kPa at the natural soil, which combined with the 400 $\mu\varepsilon$ strain suggests that the E-moduli of the cement–soil and natural soil were 300 and 75 MPa, respectively. The 300 MPa E-modulus sounds reasonable for a cement–soil mix, but a 75 MPa E-modulus would be large for clay and silt. The stress cells might have been placed on an appreciably thick engineered backfill layer above the natural soil.

Figure 18 shows the measured distribution of axial load in the piles at end of construction and 1 year later. I have added a hypothetical load distribution between the measured data points showing shaft resistance mobilized along the lower length of the pile from the pile toe upward along the length required for the measured shaft resistance to have developed. The hypothetical distribution follows the principle put forward by Franke (1991), who stated "When load is applied to a group of piles, the shaft resistance is not mobilized as in a single pile, from the head to the toe, but from the toe to the head."

2.11. Yamashita et al. (2011)

Yamashita et al. (2011) also presented a similar case history of a 12 storey building on a raft supported on a grid of a cement–soil wall and 45 m long, 900–200 mm diameter precast piles. The raft contact stresses measured at the end of construction were about 280 kPa at a stress cell on the cement–soil wall and about 50 kPa at the natural soil, i.e., the stiffness of the cement–soil wall was about 5 times that of the untreated soil. This suggests that the actual contact stress is linked to the stiffness of the soil where the stress measurement is made.

2.12. Kakurai et al. (1987)

Kakurai et al. (1987) reported 420 days of load measurements on 24 m long, driven pipe piles under a piled raft supporting a silo building. Figure 19 shows the distribution measured at the pile head and two levels down an interior pile. The authors connected the data points with straight lines. I believe that the dashed line marked "Alt. 1" indicates a qualitative distribution of the lower pile length affected by shaft resistance as the pile is pushed into the soil at the pile-toe level, again mobilizing shaft resistance along the lower length of the pile from the pile toe upward. As it is likely that the axial pile loads in the driven piles are affected by residual load, the dotted line marked "Alt. 2" is a qualitative dis-

Fig. 18. Distribution of axial pile load in an interior pile at end of construction and 1 year later together with the soil layering and distribution of SPT-N indices (data from Yamashita et al. 2013).
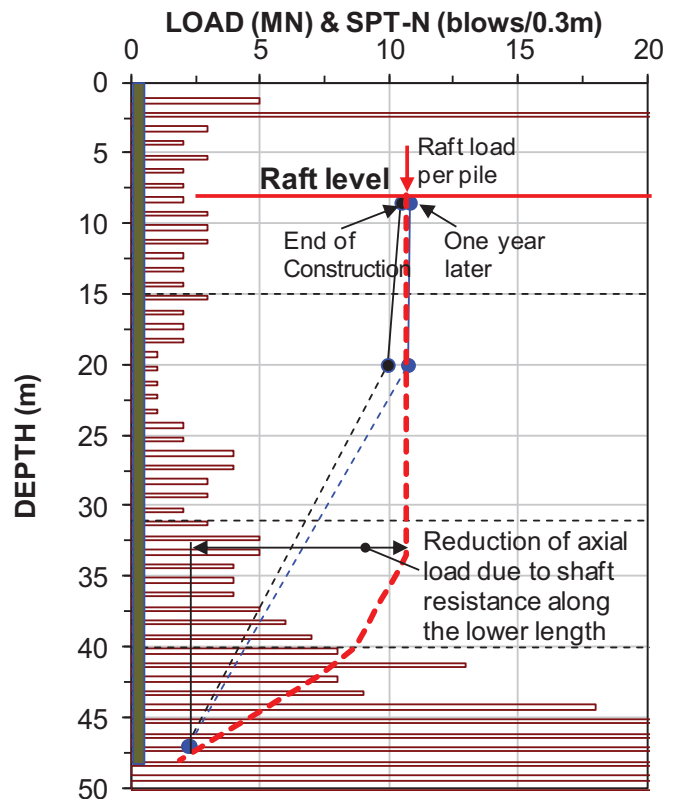
tribution adjusted for assumed residual load not included in the measured data point near the pile toe.

2.13. Okabe (1977)

Okabe (1977) reported results from a series of investigations undertaken to study the effect of drag force on piles supporting a bridge pier in a low-lying wet paddy field. The piles were driven through a soft compressible sandy silt to about 40+ m depth. The area was undergoing regional subsidence and was expected to settle additionally due to fill being placed across the site. The piled raft had an octagonal footprint and was supporting a 30 MN bridge pier on 38 piles. The piles were 700 mm diameter, 40 m long, closed-toe steel pipe piles, joined by a common cap and the average sustained load was 800 kN/pile. The load is light; the axial

Fig. 19. Distribution of axial pile load in an interior pile (test data from Kakurai et al. 1987).

Fig. 20. Layout of piles for pile-group study (data from Okabe 1977).

Fig. 21. Load distribution in the three interior and perimeter piles and in the reference single pile (data from Okabe 1977).
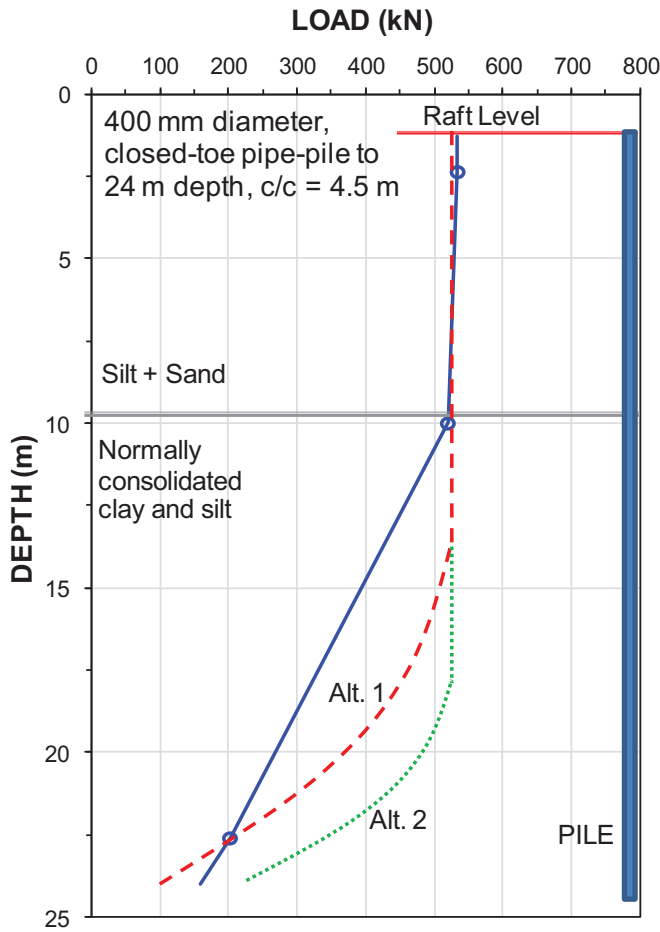
strain induced by 800 kN is about 100 to 200 με. While it is likely that the pile cap was in contact with the ground, no measurement of contact stress was reported.

The piles were placed equilaterally with a 1.5 m, i.e., 2.1 pile diameter, center-to-center spacing (18% Footprint Ratio). The layout is shown in Fig. 20, indicating the location of four test piles for which axial strain was monitored and evaluated to axial pile load at four depths over 1040 days. Three of the test piles were interior piles and one was a perimeter pile. A fifth test pile, a single 600 mm diameter, closed-toe steel pipe pile, was driven away from the group and to 43 m depth into dense sand to serve as a reference pile. It also was instrumented.

Figure 21 shows the load distributions in test piles. The distributions in the three interior piles were quite similar to each other, but differed considerably from the perimeter and reference piles.

Note that, while the perimeter pile was fully affected by the settling soil and showed the same "negative-skin-friction" development as the single pile, the interior piles did not show a similar build-up of drag force. In fact, they did not show any change of axial load, which means that the load at the pile head transferred downward without any reduction due to shaft resistance, but for a short distance above the pile toe. That is, shaft resistance was mobilized from the pile toe upward.

The long-term effect of negative skin friction developing along perimeter piles means that perimeter piles are unloaded and load is transferred to the interior piles. In the reported case, the load on the perimeter pile turned negative (by about 700 kN), i.e., a drag force developed that was larger than the working load on the pile.
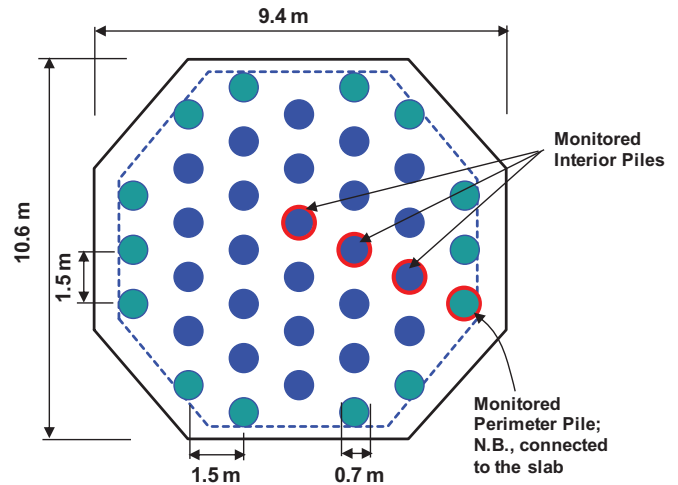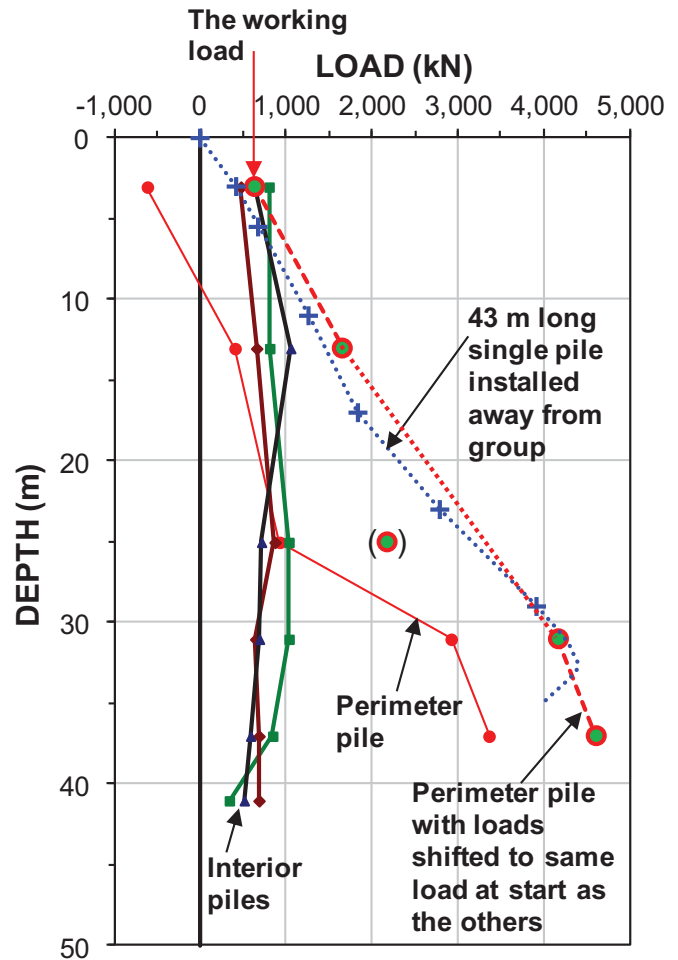
In fact, the drag force on the 14 perimeter piles was transferred to the 24 interior piles. The case history is often referred to as an example of a way to protect a piled foundation from drag force effect and, yes, the perimeter piles did shield the interior piles from drag force, but the full drag force acting on these piles was

Fig. 22. Forces on a piled raft (after Katzenbach and Choudhury 2013).
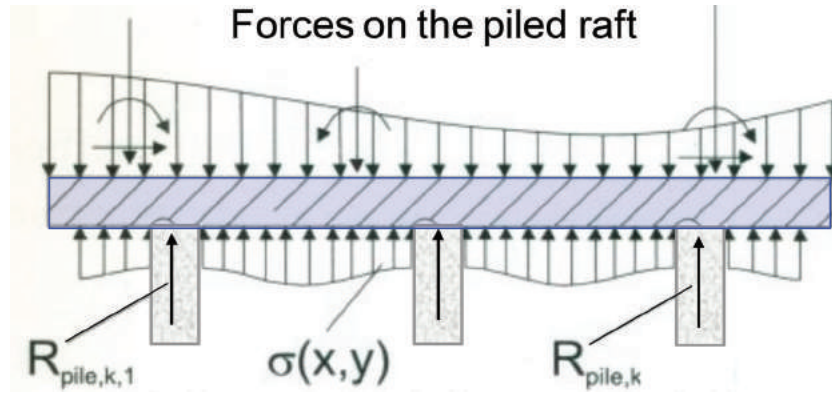
Fig. 23. Forces on piles and soil (after Katzenbach and Choudhury 2013).
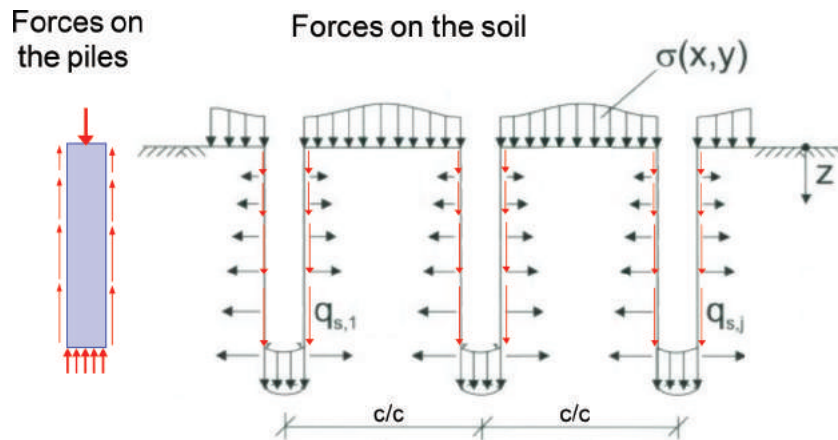
transferred to the interior piles — a not particularly satisfactory solution.

The study was directed toward the drag force, which, in the state-of-the-practice of the times, was considered the key factor. Unfortunately, the settlements of the pile and the soil were not measured (reported).

2.14. Liew et al. (2002)

Liew et al. (2002) presented a case history on a 17.5 m wide oil storage tank over soft compressible organic clay supported on 350 mm diameter spun piles — the tank center had 21 piles, 36 m long, next were two rows of 68 piles 24 m long, and along the perimeter were two rows of 68 piles, 24 m long; 137 piles in all. The average pile spacing was 1.7 m and the Footprint Ratio was 4.8%. A hydro test to a total load of 25 MN (100 kPa average stress) was performed on the tank and the settlements across a diameter were measured. An about 1 m high sand fill was placed on the ground under the raft footprint to raise the raft above the water table, which caused some settlement of the soil around the piled foundation. The purpose of having the perimeter pile shorter was to reduce dishing of the raft; that is, reduce the differential settlement. The hydro test resulted in a 26 mm settlement in the center of the tank. Along the tank perimeter, the settlement ranged from 15 to 19 mm. The authors also found that the shorter perimeter piles received less load than the longer interior piles — the loads ranged from 100 to 150 kN, while the load measured for the 36 m interior piles ranged from 300 to 400 kN. The transfer of load from the perimeter piles to the interior piles is due to the combined effect of the softer axial stiffness response of the shorter perimeter pile in relation to the longer interior piles and to the effect of the settlement around the foundation. The paper does not provide

sufficient information to allow estimating how much of the unloading is due to one or the other condition.

3. Comments

3.1. Usual comprehensive numerical analysis of wide pile group response

The more sophisticated methods of analyzing the response to load by a pile group — wide or narrow — is typically that shown by Katzenbach and Choudhury (2013) in a guideline produced on behalf of the ISSMGE Committee TC212 for the analysis of a piled-raft foundation as a "combined pile-raft foundation (CPRF)" as illustrated in Figs. 22 and 23. Also available in Katzenbach et al. 2012). The first figure shows the forces acting on the raft: the applied load (stress across the raft), the pile reaction, and the contact stress. The second shows the forces on the soil: the contact stress, and the shaft and toe resistances.

It is important to note that the method asserts that shaft resistance (*i*) acts on all the piles of the pile group — on perimeter piles as well as on interior piles, (*ii*) develops along the full length of the piles, and (*iii*) increases with depth as were it governed by an overburden effective stress relation. Moreover, additional resistance to support the foundation is assumed to be derived from contact stress over the area between the piles.

Figures 22 and 23 ostensibly represent mobilization of ultimate pile resistance. Only rarely does similar representation include the forces that act on the soil below the pile toe level and even less common is an indication of forces resulting from working load conditions as opposed to showing forces at perceived ultimate conditions.

Fig. 24. Footprint ratio as a function of grid type and pile size vs. pile spacing. [Color online.]
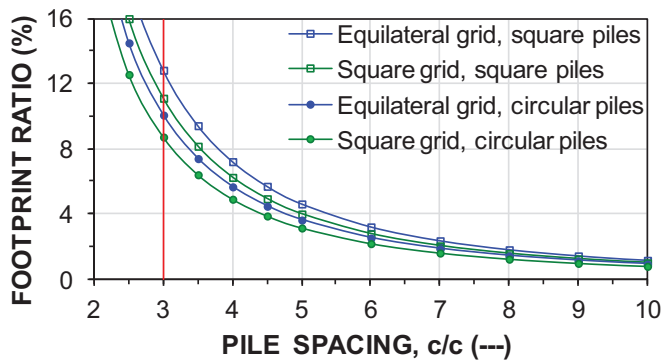
3.2. Comments on the reviewed case histories

In broad terms, the settlement of a piled foundation consists of three parts: (*i*) the compression of the body of pile and soil, (*ii*) the load-transfer movement of the pile toe into the soil, and (*iii*) the settlement below the pile-toe level due to the load imposed from the pile group.

In analyzing the compression of the body of pile and soil, usually referred to as equivalent-pier analogy, a pier E-modulus is determined by combining the E-moduli of the pile and soil body, as expressed in eq. (1). Because the E-modulus of the pile material is either 200 GPa (steel piles), about 30 GPa (concrete piles) or about 5 GPa (wood piles) and that of the soil is rarely more than about 50 MPa and frequently much smaller, the soil modulus has negligible influence on the pier stiffness (*EA*), which therefore depends mainly on the pile E-modulus and spacing (i.e., the Footprint Ratio). N.B., the Equivalent Pier analogy postulates strain compatibility.

$$(1) \qquad E_{\text{pile+soil}} = \text{FR}(E_{\text{pile}}) + (1 - \text{FR})E_{\text{soil}} \approx \text{FR}(E_{\text{pile}})$$

where $E_{\text{pile+soil}}$ is the combined E-modulus; FR is the footprint ratio (= $A_{\text{pile}}/A_{\text{raft}}$); E_{pile} is the E-modulus of the pile; E_{soil} is the E-modulus of the soil; A_{pile} is the cross-sectional area of piles; A_{raft} is the footprint area of the raft.

The compression contribution to the foundation settlement is then expressed in eq. (2) as the shortening of a pier with height, *H*, when loaded by a total load, *Q*, and as a function of the Footprint Ratio (FR).

$$(2) \qquad \Delta L = \frac{QH}{E_{\text{pile+soil}}A_{\text{raft}}}$$

where ΔL is the compression contribution to the settlement; *Q* is the load applied to the foundation raft; *H* is the height of the Equivalent Pier (length of piles); $E_{\text{pile+soil}}$ is the combined E-modulus; A_{raft} is the footprint area of the raft.

The Footprint Ratio is the ratio between the total area of all piles over the footprint area of the pile group defined by the envelop around the piles. (N.B., the shape of the pile raft is irrelevant.) The Footprint Ratio depends mainly on the spacing and marginally on the pile shape being circular or square and whether the piles are placed in equilateral or square grid. A group of circular piles placed symmetrically at a spacing of 3 pile diameters in a wide foundation (equilateral or triangular configuration) has an FR of 10.1%, whereas the FR is 8.7% for the piles placed at a 3 diameter spacing in a square grid. Figure 24 shows the relation between the Footprint Ratio and pile spacing for circular and square piles placed in equilateral and square grids. As the piles in a group are often not uniformly distributed, the simplest approach is to determine the Footprint Ratio from the area of all piles over the total footprint area.

Equation (3) shows the strain, ε, induced in the piles and in the soil by an applied load, *Q*. The compression is simply obtained as the strain times the height of the pier, the pile embedment length.

$$(3) \qquad \varepsilon = \frac{Q}{E_{\text{pile+soil}}A_{\text{Raft}}}$$

where ε is strain; *Q* is the load applied to the foundation raft; $E_{\text{pile+soil}}$ is the pier E-modulus; A_{raft} is the footprint area of the raft.

The case histories by Broms (1976), Golder and Osler (1968), Badellas et al. (1988), Goossens and van Impe (1991), van Impe et al. (2013), and Gwizdala and Kesik (2015) show that the simple concept of the Equivalent Pier and an equivalent flexible raft at the pile toe level combined with appropriate compressibility soil parameters and Boussinesq distribution of stress can model not just the average settlement of the raft, but the distribution of settlement across the raft (dishing) and the influence of the pile raft also outside the raft footprint and, indeed, the interaction between adjacent piled rafts.

The concept of the Equivalent Pier goes beyond estimating the compression of the pile and soil body. The pile and the soil work in unison very much the same way as the rebars and the concrete work in a reinforced concrete column. When load is applied to the top of the concrete column, the resulting axial stresses in the rebars and in the concrete develop in proportion to the moduli of the materials (steel and concrete) and their respective areas of the column cross section. If down the pile a crack exists cleanly across the column, then all load will be in the rebars. Further down, when again the column is sound, the distribution between the rebar and concrete is back to what it was at the head. If at the base of the column the rebars protrude a small distance, all load is back in the rebars and, if the base is soft, the rebars might start to penetrate into the base (the "floor") and they will do so until the penetration is equal to the rebar protrusion, which is when the concrete starts to experience stress and the rebars, therefore, start to unload. Then, further penetration of the rebars might cease. If concrete — the matrix — would not be concrete, but some soft material and the rebars not be protruding, then, they could still be pushed into the base, the floor as it were, provided that the matrix around the rebars would be compressed as much as the rebars are pushed into the base.

Just like the rebars and the concrete in the reinforced concrete column, the distribution of the raft load to the piles and to contact stress is according to the respective E-moduli of the piles and the soil and to the respective areas of pile and soil. The strain in the pile and in the soil must be equal. Ordinarily, the strain introduced in the pile by the working load can amount to about 200 µɛ, which, for say, a 400 mm diameter square concrete pile, correlates to a load of about 800 kN. Most soils surrounding a pile would have a modulus that is three to four orders of magnitude smaller than the modulus of the pile material. Thus, a 200 µɛ soil strain combined with, say, a soil E-modulus of 50 MPa, will amount to 10 kPa stress, contact stress if considered directly under the raft. Coincidentally, the contact stress is about equal to the "wet load" of the concrete raft. At, say, a 5 m² footprint area per pile, this correlates to 50 kN load — "contact raft load" — from the raft to the soil over the pile footprint portion of the raft. This does not mean that the contact raft load can be assumed to be load taken off the piles — a common mistaken assumption. Strain compatibility requires, for example, that, if deeper down, the soil matrix is very compressible (say, the pile goes through a layer of soft clay), load in the soil would be transferred to the piles increasing the strain — and stress — in the pile (and strain, but not stress, in the soil) until a new level of compatibility or strain equilibrium is established. Then, in the, say, stiff soils further down, the reverse happens: load is transferred from the pile to the soil until strain

equilibrium is again established. These changes occur with minimum of relative movement between the pile and the soil.

The foregoing means that a uniformly distributed load applied to a piled raft will impose an average strain in pile and soil that will not change with depth (provided that the relative stiffness pile to soil remains the same). That is, not change until down to the zone where the effect of the pile-toe boundary has worked itself upward from the pile-toe level.

At the toe of the pile, when it is being pushed into the soil, the matrix — the soil around the pile — will compress and the lower boundary of the matrix will move upward a distance equal to the pile toe penetration. The toe penetration is equal to the compression of the soil upward from the pile toe level. The compression causes a relative movement to develop between the pile and the soil immediately above the pile toe, generating shaft resistance starting from the pile toe upward. When the toe penetration is short (small), the length of pile above the pile toe with shaft resistance is short. For piles in soft soils, the matrix compression can be large and, therefore, result in a long length of pile with shaft resistance. This appears to have been the case for the two buildings supported on piles in soft clay reported by Hansbo 1984.

The piles inside a pile group will interact much like the interaction and interplay of stress between the reinforcement and the concrete in a reinforced concrete element. However, any axial force that is shed to the soil is then transferred from the soil to a neighboring pile that, in turn, sends some of its own force to the first pile or to other piles. Performing a static loading test on a pile, Caputo and Viggiani (1984) and Lee and Xiao (2001) showed that the adjacent piles moved, too, demonstrating that a significant interaction can develop between adjacent piles.

The toe penetration is governed by the stiffness of the soil matrix immediately above the pile toe level and by the stiffness of the soil below. This penetration is the load-transfer movement of the pile group.

Where no long-term subsidence is expected, the fact that the response of perimeter piles is stiffer than that of interior piles and that, therefore, perimeter piles settle less than interior piles, results in dishing of the raft and differential settlement. As shown by Liew et al. (2002) and recommended by Katzenbach and Choudhury (2013), the differential settlement can be offset by making the perimeter piles shorter than the interior piles, which makes the response of the perimeter pile less stiff and the settlement of the perimeter area more like that of the interior area; that is, reduces dishing, the raft differential settlement. In contrast, where long-term subsidence is expected, the solution is to instead lengthen the perimeter piles.

4. Analysis example

The results of the case history survey can be illustrated by the following hypothetical example of a wide piled-raft foundation supported on 350 mm diameter, circular concrete piles driven into a sandy silt to 15 m depth. Figure 25 shows typical results of a static loading test on a single pile (load–movement curves for the pile head, pile toe, pile shaft, and pile compression). The test curves are derived from a numerical fit to an actual test. The raft will have a 350 kPa uniform stress (including the weight of the raft). Four alternative designs are considered. Alternatives 1 and 2 pertain to conventional design with working pile loads of 600 and 900 kN, respectively, and, as conventionally assumed, no support from raft load (raft–soil contact stress) is considered available.

Alternatives 3 and 4 are pile-enhanced raft designs with working pile loads equal to 1400 and 2000 kN, respectively. The raft contact stress is as required by strain compatibility.

The raft is wide and the piles will be placed in a square grid. The E-moduli of the pile and the soil are 30 GPa and 40 MPa, respectively.

Fig. 25. Results of a static loading test on a 350 mm diameter, 15 m long pile.
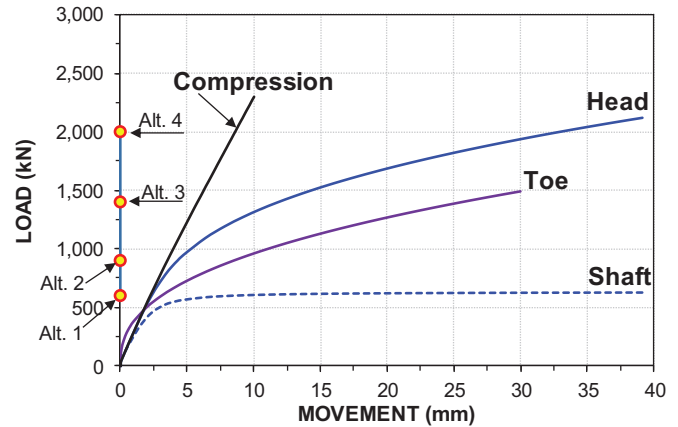
Alternatives 2 and 3 are realistic, while Alternative 1 is somewhat uneconomical and Alternative 4 is, say, unusual. Each assumed working load determines the affected Footprionot Ratio (and pile spacing). Despite of the mentioned assumption that Alternatives 1 and 2 are per "conventional design," i.e., that all raft load would be supported by the piles, the fact is that raft contact stress will occur also for these alternatives.

The common approach is to designate a pile "capacity" from the static loading test according to some definition (of which there are many in use), and apply some assigned factor of safety to arrive at an allowable load and call this the pile working load, which determines the number of piles supporting the raft (and pile spacing). Conventional design disregards contribution from the raft "bearing capacity", while contact stress is included for a piled raft or pile-enhanced raft, usually as a stress determined by a factor of safety applied to the raft "bearing capacity". This approach is not correct, however. The separation of the load between the piles and the raft can only be established from the requirement for strain compatibility, considering working load conditions as opposed to "capacity", and recognizing the fact that the pile axial stress and the soil contact stress depend on the stiffness interaction of pile and soil.

The correlations for the four alternative working loads are compiled in Table 2. The table pertains to flexible and rigid rafts alike and to interior piles of the wide group, showing the calculated pile strain, pile spacing, Equivalent Pier modulus, contact stress, and ratio of load on the soil to the pile load. For each alternative four lines at the bottom of the table list the pile toe resistance, the pile compression, the load-transfer movement, and the raft settlement above the pile toe level. The raft settlement is made up of the pile compression and the load-transfer movement. Each is determined per the process illustrated in Fig. 26 for the 1400 kN pile working load, where the toe-resistance curve is the one established in the static loading test. The curve labeled "Total load minus the shaft resistance above the pile toe" is calculated after subtracting from the applied load the shaft resistance mobilized along a length of pile extending upward from the pile toe for a movement equal to the pile-toe movement. The curve labeled "Toe Resistance" is the pile toe resistance response for the pile-toe movement; the same curve as that shown in Fig. 25. The intersection of the two curves is where the total axial load reduced and where the shaft resistance above the pile toe is equal to the toe resistance. The process also identifies the length of pile engaged above the pile toe by the dashed curve showing the length of the pile with shaft resistance mobilized above the pile toe due to the toe movement.

I have assumed that the distribution of shaft resistance along the lower length of the pile is the same as that for the test pile. In

Table 2. Results from combining load with pile and soil E-moduli.

Parameter	Alternative 1	Alternative 2	Alternative 3	Alternative 4
Working load (kN/pile)	600	900	1400	2000
Strain in pile and soil ($\mu\varepsilon$)	250	370	580	830
Average pile spacing (m)	1.3	1.6	2.0	2.4
Average pile spacing (diameter)	7.7	5.2	6.4	7.7
E-modulus for Equivalent Pier (MPa)	1450	980	650	470
Contact stress (kPa)	12	19	29	42
Soil-load to pile-load ratio (%)	3	5	9	12
Mobilized toe resistance (kN)	500	600	1200	1500
Compression of pier (mm)	2	5	9	12
Load-transfer movement (mm)	2	6	16	30
Compression and load transfer (mm)	4	9	22	40

Fig. 26. Process for determining the load-transfer movement for 1400 kN working load (Alt. 3).
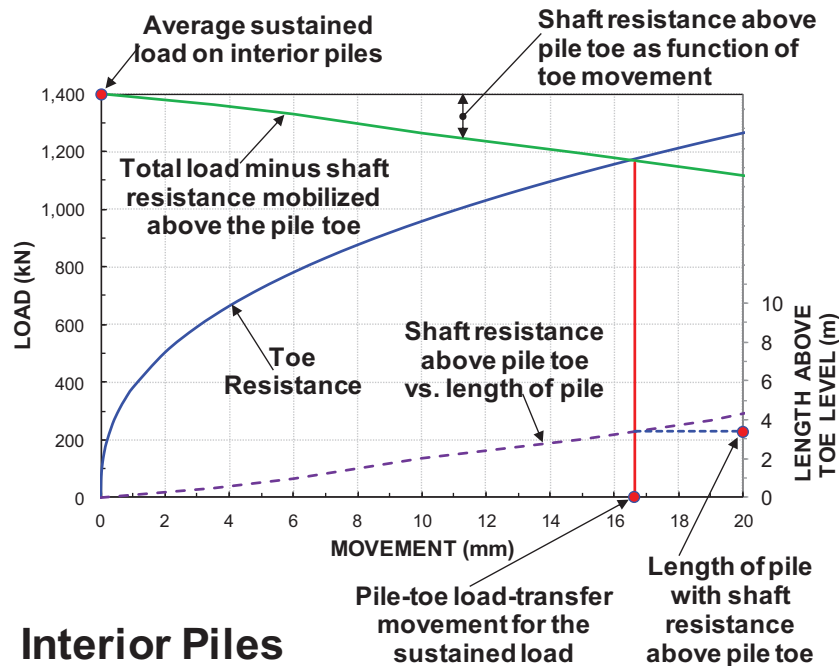
Interior Piles

reality, however, I would expect that the fact of the soil being confined between the piles would result in a stiffer soil response than that shown by the static test on the single pile. Assuming the same conditions for interior and single piles, the group is conservative, inasmuch it would result in smaller load-transfer movements. I am not aware of any full-scale test data that could verify this, however. N.B., the raft is considered wide and the discussion pertains to the interior piles only, leaving the perimeter piles on the side, as it were.

Figure 27 compiles the results for the four alternatives and shows the contact stress, the soil–pile load ratio, and the settlement of the raft above the pile-toe level (the sum of pier compressions and pile-toe load-transfer movements is also shown). N.B., the settlement contribution from the compression of the soils below the pile toe level is not included. Depending on the specific conditions of the site, it could be small or large. However, it would only depend on the average raft stress, which is the same for all three alternatives. It is therefore not addressed in this figure.

The curves show that as the load per pile is increased, also the soil–pile ratio (load on soil to load on piles) increases, as does the contact stress. The figure makes it clear that there is no difference in principle between the conventional raft and the pile-enhanced raft or pile raft response. Indeed, this statement applies also to a raft elevated above the ground; a few metres below the ground,

strain compatibility requires that the soil is stressed per the requirement of having the same strain as that of the pile.

Figure 28 compares the load distribution for single and interior piles of Alternative 3 calculated by applying effective stress principles using the UniPile software (Goudreault and Fellenius 2014). The load distribution of the interior piles is similar to those from the referenced full-scale measurements (cf., Figs. 18 and 19).

It is obvious that the strain-compatibility approach indicates that, for interior piles, the shaft resistance in the upper length of a pile has little impact on the response of the piles supporting a piled raft. Ordinarily, even the shaft resistance near the pile toe is less important than the pile-toe response; that is, the pile-toe response determines the load-transfer movement. Of course, in the case of essentially shaft-bearing piles having minimal toe resistance, the length engaged above the pile toe would depend only on the shaft resistance along some length of the pile up from the pile toe. Assume, for example, that the shaft resistance response is plastic with the unit resistance increasing with depth according to either a constant value (total stress; undrained shear strength) or, more realistically, increases by the principles of effective stress. Then, if the applied load is chosen as a third of that shaft resistance, the length of the pile shaft engaged by shaft resistance above the pile toe level would be about a third or less of the pile

Fig. 27. Contact stress load-transfer movement, compression, and settlement (left ordinate) and load per pile (right ordinate) vs. average spacing in pile diameters.
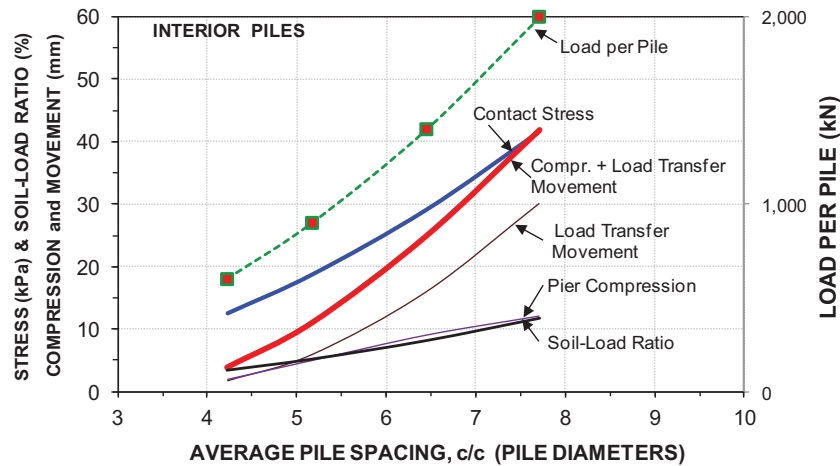
Fig. 28. Load distribution for 1400 kN applied load; single and interior piles.
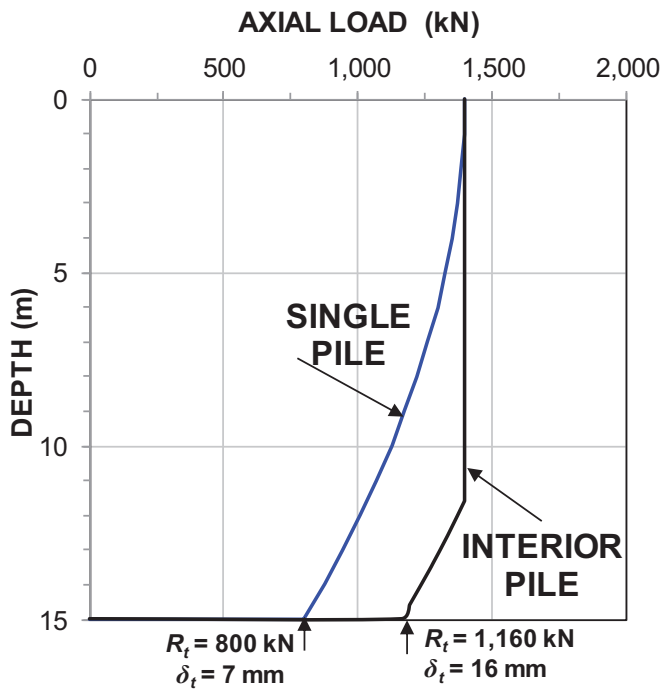
length. N.B., the assumed strain compatibility does not occur in the shaft resistance zone immediately above the pile toe level.

As the analysis behind Fig. 28 presupposes that the interior piles are engaged from the toe upward, it cannot be used to prove that the "toe up" engagement is a true model of the pile group response. The results of the UniPile analysis were therefore compared to the results of a sophisticated numerical analysis (Plaxis) by calculating the response of an 8.4 m wide raft supported on a group of 49 piles comprising the same pile type and soil. The Plaxis analysis assumed a rigid pile raft, a linear-elastic to plastic shaft resistance response (Coulomb), the same toe resistance load–movement as that used in the UniPile analysis, a 35° internal friction angle, a 0.8 earth stress coefficient (K_0), and a 40 MPa soil modulus. This set of parameters gave the same simulated load–movement response of a static loading test on a single pile as shown in Fig. 25. It is also assumed that the soil deposit was 50 m thick. The Plaxis run on the group was performed by imposing a

series of 10 mm raft movements to a 40 mm maximum settlement of the raft.

Figure 29A shows the results of the Plaxis analysis of the 40 mm maximum raft settlement, which included an average of about 25 to 30 mm settlement of the soils below the pile toe level. The pile toe movements calculated for the interior piles were about 3 to 5 mm and about 15 to 20 mm for the perimeter piles. The axial load in the interior piles was unaffected by shaft resistance until about 0.5 to 1 m above the toe of the interior pile. In contrast, the perimeter piles were affected by shaft resistance from the pile head down, the corner pile response being similar to that of a single pile. The process for determining the load-transfer movement shown in Fig. 26 assumed pile head load of 1400 kN. If, instead, the curve showing the "total load minus shaft resistance above the pile toe" would be moved down to start from the 900 kN load (the Alternative 2 condition), the subsequent intersection and construction would indicate a length affected above the pile toe of about 0.5 m. Moreover, as shown in Fig. 27, the settlement of the raft due to pier compression and pile-toe load-transfer was 18 mm, which is essentially the same as the 20 mm average of the Plaxis analysis. Thus, the main results of the toe analyses are satisfactorily similar.

The relative movement between the pile and the soil is the difference between the soil settlement and the pile movement. The analysis shows that, along the interior piles down to the vicinity of the pile toe, no appreciable difference occurred. The pile toe penetrations are essentially the same for the UniPile and Plaxis analyses. It is interesting to note that, in contrast to the simple effective stress analysis, the Plaxis analysis registered the compression of the soil near the pile due to the shear force and associated stress increase.

The "capacities" and factors of safety implied in the four alternatives are very nebulous. Let me disregard the fact that the engineering practice shows neither consensus of how to define capacity nor of what factor of safety to apply and, simply, state that Alternative 2 represents a conventional design with a factor of safety equal to 2.0 and Alternative 3 represents a design for a pile-enhanced raft with a factor of safety of 1.0 applied to the pile response. The only way the two designs then can be compared is with regard to what the structure supported by the foundations would experience with one or the other. The calculation compilation in Fig. 26 shows that for Alternative 2, the conventional design, the settlement would be about 9 mm and for Alternative 3, it would be about 22 mm (disregarding all contribution from below the pile toe level). Alternative 2 would, however, require about

Fig. 29. Results of numerical analysis: (A) soil settlement and pile movement; (B) axial pile loads.
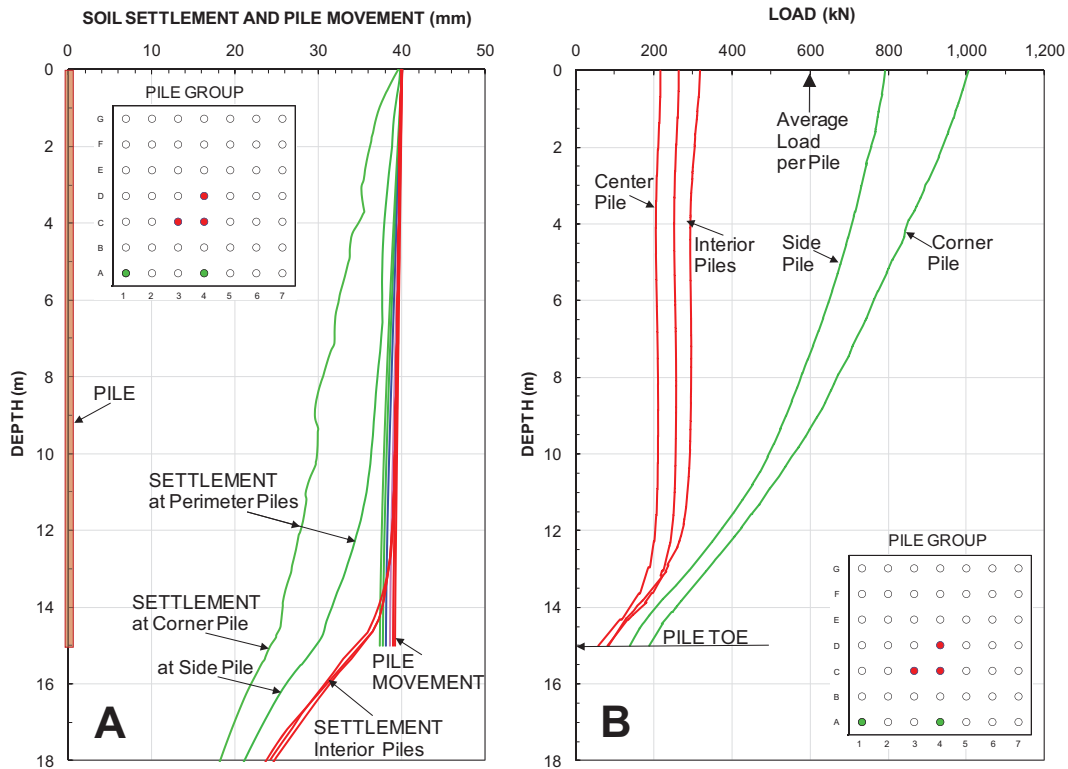
50% more piles than Alternative 3 and be correspondingly more expensive.

The contribution from contact stress is usually calculated based on a bearing capacity formula with some factor of safety applied. By this approach, for most cases, the contact stress contribution is assigned a value that goes well beyond the contact stress governed by the requirement for strain compatibility. Even the extreme case represented by Alternative 4 (c.f., Table 2) shows no more contribution from contact stress than about 12% of the pile load. Indeed, were the soil matrix to consist of very soft highly compressible soil some distance down along the pile, but still above the pile toe level, then, at that depth, practically all load would be in the piles. Similarly, if an intermediate, stiffer soil layer were to be present, the soil–pile load ratio would again change, i.e., adjust to the new stiffness conditions. Simply, a bearing capacity or strength approach applied to a combination of materials, where the composition may change, be it in geotechnical or structural design, is a flawed approach that should be removed from geotechnical engineering practice.

The foregoing has addressed the interior piles and left out the response of the perimeter piles. It must not be overlooked that, as shown by the case records reported by Okabe (1977), Russo and Viggiani (1995), and Mandolini et al. (2005), the perimeter piles behave more like single piles and they are indeed affected by shaft resistance from the pile cap level to the pile toe (cf., Fig. 27). This means that a perimeter pile experiences smaller pile compression than an interior pile and would, therefore, attract a larger portion of the load from the structure (unless the raft is ideally flexible). The net effect is still that of the pile head of the perimeter pile moving less than the head of the interior pile; that is, dishing will occur for the raft.

As mentioned, Liew et al. (2002) and Katzenbach and Choudhury (2013) recommended that the perimeter piles should be designed shorter so they settle more evenly with the interior piles. Note however, that the perimeter piles of piled foundations in subsiding soils will in the long term be subjected to downdrag and drag force. The downdrag will increase the settlement of the perimeter piles and the drag force will add load to the foundation raft, increasing the load on the interior piles, as was observed for the case history reported by Russo and Viggiani (1995). The interior piles will not be subjected to similar downdrag or drag forces. Therefore, in such conditions, the perimeter piles should instead be designed longer than the interior piles. Though, with respect to the implication on the design of the actual raft (slab) immediately after construction, the short-term condition for such a design would have to be assessed.

The rigidity of the raft is an important aspect of the design of any raft foundation inasmuch it influences the distribution of load between the piles. Whether a raft is more rigid or more flexible than another matters little for the piles, soils, and raft over the distance between the piles; the net span being equal to the c/c spacing minus a pile diameter; that is, about the same as the thickness of the raft and often less. However, over the full width of a raft, the increased raft width will have a noticeable effect on the raft bending forces (and pile head connection to the raft), but less so for the soil and for the piles down the soil. The wider a raft, the more flexible it will appear.

The actual contact stress and the portion of contact load to pile load is a function of the soil stiffness. If the piles go through a very soft soil layer, all loads will be transferred to axial force in the piles by virtue of the strain compatibility. Similarly, where the piles go through a dense soil layer, the pile axial load will reduce and the soil stress will increase. What matters for the settlement of the piled foundation is the pier modulus, the pile toe conditions, and the compressibility below the pile toe level.

If, for the ideally flexible raft, all piles are assumed to have the same working load, then the pier compression ("settlement") will be larger in the center of the raft, because the larger shaft resistance experienced by the perimeter piles will result in their experiencing a smaller compression and smaller pile-toe penetration (load-transfer movement). The flexible raft will, therefore, develop a bowl shape, i.e., experience "dishing", that is larger than that of the Equivalent Raft at the pile-toe level.

Fig. 30. (*A*) Settlement and (*B*) load distributions across a pile raft due to pier compression, load transfer, and settlement in underlying soils for ideally flexible and ideally rigid piled raft.
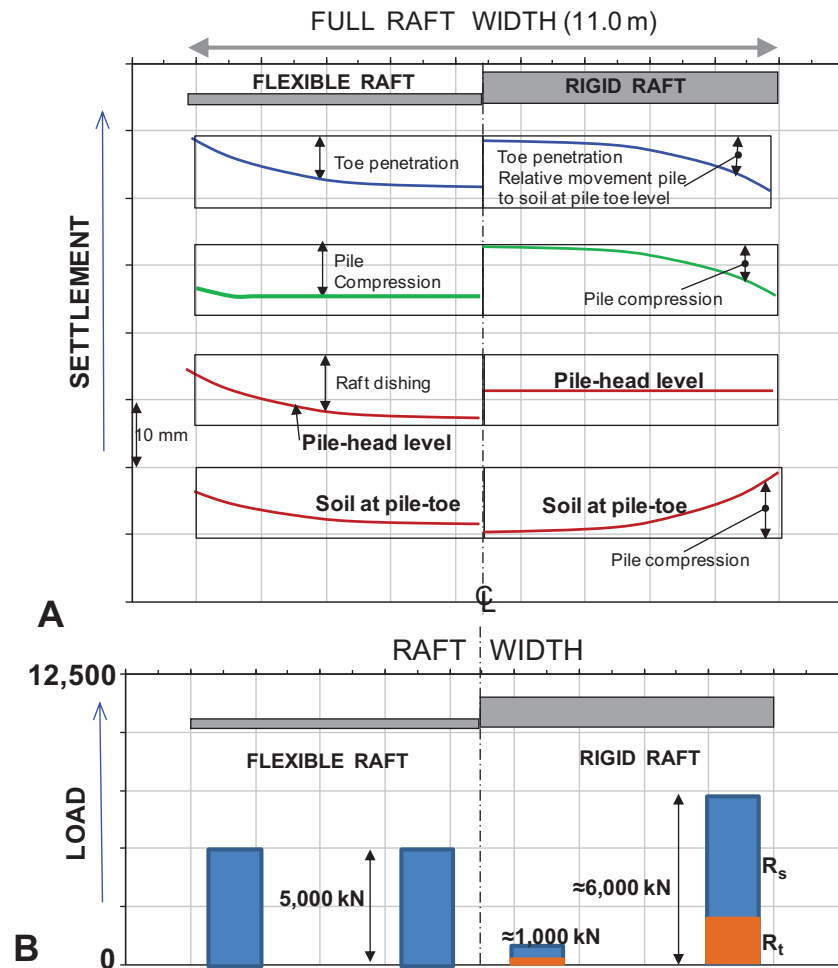

Figure 30*A* compares the typical response of an ideally flexible raft and an ideally rigid raft supporting a uniform load, here assumed to correspond to an average of 1400 kN per pile. For the flexible raft, the total settlement at the pile head level is the sum of the pile compression for the applied load (load is the same for all piles, but perimeter piles are affected by shaft resistance), the pile toe movement, and the settlement of due to the compression of the soil layer below the pile-toe level (calculated using the Equivalent Raft method). For the latter method, I have assumed soil depths and compressibilities that results in an about 10 mm differential settlement between the perimeter and the center of the Equivalent Raft. The settlement of the flexible raft was calculated applying conventional soil consolidation and compressibility parameters together with Boussinesq stress distribution. N.B., the dishing of the Equivalent Raft depends very much on the compressibility of the soil layer below the pile toe level and it will affect the distribution of pile compression and pile toe penetration.

For the ideally rigid piles, the response is more complex. Figure 29*B* shows the load distribution. I calculated the loads assuming that the load on the interior piles would reduce by 300 kN and the increase of load for the perimeter piles was then estimated based on a 1400 kN average load for the piles in the raft. This resulted in a 1900 kN load on the perimeter piles. I then calculated the resulting pile compression and toe movement for the piles. The latter is a combination of actual downward movement of the pile toe into the soil and the compression or enforced additional upward movement of the soil in-between the piles at the pile toe level.

Because the loads are smaller for the interior piles and larger for the perimeter piles, when applying the loads to a flexible raft (actually to a series of small rafts each with its working load), the distribution of compression of the soil below the pile-toe level is more even across the raft than that calculated for equal load across the raft.

The ideally rigid raft will not experience dishing and the average settlement will be smaller and about equal to the settlement at the characteristic point (Steinbrenner 1934, 1936; Kany 1959), plus the pile compression and load transfer movement for each pile location.

The calculations behind Figs. 29*A* and 29*B* are qualitative and mainly intended to show the difference between the interior and perimeter piles for flexible and rigid piled raft. A real-world raft can neither be ideally flexible nor ideally rigid. For a wide piled raft, the response is likely more similar to that of a flexible raft than to a rigid one, however.

The compression and the load transfer for the interior piles were calculated as indicated in the foregoing, while the perimeter piles were assumed to respond similarly to the single pile, which determined their compression and load transfer. The distribution between the perimeter and the center was drawn by assuming a gradual change. Further analysis would require numerical work matched to actual measurements of movement and strains in the pile and soil, at the pile head and down to the pile toe, for both interior and perimeter piles, and include measurements of bend-

ing forces in the raft. The currently available case records are not even close to providing such reference data.

5. Conclusions

The survey of cases histories reporting observations of full-scale response of wide pile groups, primarily with regard to the interior piles, has shown that a simple equivalent-pier analysis satisfactorily models the compression of the body made up of piles in a matrix of soil, and the equally simple assumption of an Equivalent Raft placed at the pile-toe level satisfactorily models the settlement of the soils underneath the pile toe-level. These models are part of the existing geotechnical toolbox.

The pile and the soil will experience equal strain from the applied load as determined from the pier E-modulus, which is the raft Footprint Ratio times the pile E-modulus. The contact stress is a function of that strain in combination with the E-modulus of the soil underneath the raft.

The survey also shows that for interior piles in a group, the transfer of applied load develops from the pile toe upward in contrast to that of single and perimeter piles, where it develops from the ground downward.

The latter observation can be modeled by calculating the load at the pile toe remaining after shaft resistance has reduced the axial load in the pile, starting from the pile toe level. When the so-calculated load is equal to the known pile toe resistance, the actual load distribution in the pile is determined and the load-transfer movement of interior piles is equal to the toe movement for that toe resistance.

It follows that knowing the pile toe response is a key aspect of a piled foundation analysis and, therefore, in the planning, execution, and analysis of a static loading test.

The response of perimeter piles (outer rows) is similar to that of single piles. In a non-subsiding soil profile, the differential settlement and bending force in the raft can be reduced by shortening the perimeter piles in regard to the interior piles. However, where the soils at the site are subjected to ongoing settlement from general subsidence, fill or adjacent structures, it may be advisable to instead lengthen the piles. Which approach would be most suitable depends on the specific conditions and must be analyzed separately for each case.

The requirement for compatibility between the strain in the piles and the soil governs the relevant load between the pile and the soil (contact stress) and indicates that the interior piles are not subjected to drag force and downdrag in areas of general subsidence in contrast to the perimeter piles and single piles.

The distinction frequently made between piled raft solely deriving bearing from the piles and pile-enhanced raft is artificial. While the geometry, pile spacing, and applied load per pile ensures smaller contact load for the former and larger contact load for the latter, there is no difference in principle and no bearing contribution is provided by the contact stress. Indeed, a piled foundation with elevated piles will not respond in any different manner to that of a piled foundation with the raft placed on the ground.

The settlement of a foundation is the deciding aspect of a design. The common approach of designing for a factor of safety applied to a capacity — of a sort — does not correctly model the degree of satisfactory response of a foundation. This uncertainty both results in excessive costs of piled foundations and inadequate safety.

Future studies of the response of a piled raft to load should include measuring not contact stress, but soil strain along with the strain in the piles and this at several depths, most important, near the pile toe level, where also the movement difference between the pile and the soil should be recorded. It will be very important to measure these parameters at interior piles as well as at perimeter piles.

References

Auxilia, G.B., Burke, P., Duranda, M., Ulini, F., Buffa, L, Terrioti, C., Dominijanni, A., and Manassero, M. 2009. Large storage capacity cement silos and clinker deposit on a near-shore sandy fill using piles for soil improvement and settlement reduction. *In* Proceedings of the 17th International Conference on Soil Mechanics and Geotechnical Engineering (ICSMGE), Alexandria, 5–9 October 2009, Vol. 3, pp. 1181–1184. doi:10.3233/978-1-60750-031-5-1181.

Badellas, A., Savvaidis, P., and Tsotsos, S. 1988. Settlement measurement of a liquid storage tank founded on 112 long bored piles. *In* Proceedings of the Second International Conference on Field Measurements in Geomechanics, Kobe, Japan, Balkema, Rotterdam, pp. 435–442.

Broms, B.B. 1976. Pile foundations—pile groups. *In* Proceedings of the 6th ECSMFE, Vienna, Vol. 2.1, pp. 103–132.

Caputo, V., and Viggiani, C. 1984. Pile foundation analysis: a simple approach to nonlinearity effects. Rivista Italiana di Geotecnica, **18**(2): 32–51.

Fellenius, B.H. 2014. An instrumented screwpile load test and connected pile-group load-settlement behavior. Discussion. Journal of Geo-Engineering Sciences, IOS Press, **1**(2): 101–108. doi:10.3233/JGS-130014.

Fellenius, B.H. 2016. The unified design of piled foundations. The Sven Hansbo Lecture. *In* Proceedings of Geotechnics for Sustainable Infrastructure Development, Geotec Hanoi 2016. *Edited by* P.D. Long. Hanoi, 23–25 November, pp. 3–28.

Franke, E. 1991. Measurements beneath piled rafts. *In* Proceedings of the International Conference on Deep Foundations, Ecole National des Ponts et Chaussees, Paris, 19–21 March, pp. 599–626.

Georgiadis, M., Pitilakis, K., Tsotsos, S., and Valalas, D. 1989. Settlement of a liquid storage tank founded on piles. *In* Proceedings of the 12th International Conference on Soil Mechanics and Foundation Engineering, Rio de Janeiro, 13-18 August, Vol. 2, pp. 1057–1060.

Golder, H.Q., and Osler, J.C. 1968. Settlement of a furnace foundation, Sorel, Quebec. Canadian Geotechnical Journal, **5**(1): 46–56. doi:10.1139/t68-004.

Goossens, D., and van Impe, W.F. 1991. Long-term settlement of a pile group foundation in sand, overlying a clayey layer. *In* Proceedings, 10th European Conference on Soil Mechanics and Foundation Engineering, Firenze, 26–30 May, Vol. I, pp. 425–428.

Goudreault, P.A., and Fellenius, B.H. 2011. UniSettle, Version 4, tutorial with background and analysis examples. UniSoft Geotechnical Solutions Ltd. Available from www.UniSoftLtd.com.

Goudreault, P.A., and Fellenius, B.H. 2014. UniPile Version 5, user and examples manual. UniSoft Geotechnical Solutions Ltd. Available from www.UniSoftLtd.com.

Gwizdala, K., and Kesik, P. 2015. Pile group settlement, methods, examples of calculations referred to measurement results carried out in field tests. *In* Proceedings of the 16th International Conference on Soil Mechanics and Geotechnical Engineering (ICSMGE), Edinburgh, 13–17 September, pp. 1091–1096.

Hansbo, S. 1984. Foundations on creep piles in soft clays. *In* The First International Conference on Case Histories in Geotechnical Engineering, St. Louis, 6–11 May 1984, pp. 259–264.

Hansbo, S. 1993. Interaction problems related to the installation of pile groups. *In* Proceedings of the 2nd International Geotechnical Seminar on Deep Foundations on Bored and Auger Piles, Ghent, 1–4 June 1993, pp. 119–130.

Hansbo, S., and Jendeby, L. 1998. A follow-up of two different foundation principles. *In* Proceedings of the Fourth International Conference on Case Histories in Geotechnical Engineering, St. Louis, 9–12 March, pp. 259–264.

Kakurai, M., Yamashita, K., and Tomono, M. 1987. Settlement behavior of piled raft foundations on soft ground. *In* Proceedings of the 8th Asian Regional Conference on SMFE ARCSMFE, Kyoto, 20–24 July 1987. Vol. 1, pp. 373–376.

Kany, M. 1959. Beitrag zur berechnung von flachengrundungen. Wilhelm Ernst und Zohn, Berlin [as referenced by the Canadian Foundation Engineering Manual, 1985.]

Katzenbach, R., and Choudhury, D. 2013. ISSMGE Combined piled-raft foundation guideline. Technische Universitat Darmstadt, Institute and Laboratory of Geotechnics, Darmstadt.

Katzenbach, R., Ramm, H., and Choudhury, D. 2012. Combined pile-raft foundations— a sustainable foundation concept. *In* Proceedings of the Ninth International Conference on Testing and Design Methods for Deep Foundations, Kanazawa, 18–20 September.

Lee, K.M., and Xiao, Z.R. 2001. A simplified nonlinear approach for pile group settlement analysis in multilayered soils. Canadian Geotechnical Journal, **38**(5): 1063–1080. doi:10.1139/t01-034.

Liew, S.S., Gue, S.S., and Tan, Y.C. 2002. Design and instrumentation results of a reinforced concrete piled raft supporting 2500-tonne oil storage tank on very soft alluvium deposits. *In* Proceedings of the 9th International Conference on Piling and Deep Foundations, 3–5 June, Nice, pp. 263–269.

Mandolini, A., Russo, G., and Viggiani, C. 2005. Pile foundations: experimental investigations, analysis, and design. *In* Proceedings, 16th International Con-

ference on Soil Mechanics and Geotechnical Engineering (ICSMGE), 12–16 September, Osaka, Japan, pp. 177–213.

Okabe, T. 1977. Large negative friction and friction-free piles methods. *In* Proceedings of the 9th International Conference on Soil Mechanics and Foundation Engineering (ICSMFE), Tokyo, 11–15 July. Plenum Publishing Corporation, Berlin, Vol. 1, pp. 679–682.

Russo, G., and Viggiani, C. 1995. Long-term monitoring of a piled foundation. *In* Proceedings of the Fourth International Symposium on Field Measurements in Geomechanics, Bergamo, pp. 283–290.

Savvaidis, P. 2003. Long-term geodetic monitoring of the deformation of a liquid storage tank founded on piles. *In* Proceedings of the 11th FIG Symposium on Deformation Measurements, Santorini, Greece, 25–28 May 2003.

Steinbrenner, W. 1934. Tafeln sur Setzungberechnung. Die Strasse, **1**: 221.

Steinbrenner, W. 1936. A rational method for the determination of the vertical normal stresses under foundations. *In* Proceedings of the 1st International Conference on Soil Mechanics and Foundation Engineering (ICSMFE), Harvard. Vol. 2, pp. 142–143.

van Impe, P.O., van Impe, W.F., and Seminck, L. 2013. Discussion of an instrumented screw pile load test and connected pile group load settlement behavior. Journal of Geo-Engineering Sciences, IOS Press, **1**(1): 13–36. doi:10.3233/JGS-130011.

van Impe, W.F., and Bottiau, M. 2016. A case study of large screw pile groups behavior. *In* Proceedings of the Symposium on Pile Design and Displacement, 27 May, den Hague, 74 p.

van Impe, W.F., van Impe, P.O., and Manzotti, A. 2018. Pile design and group behaviour—a case study of large tank foundations in soft soil conditions. Geotechnical Engineering Journal of the SEAG & AGSSEA, **49**(1): 15–29.

Yamashita, K., Hamada, J., and Takeshi, Y. 2011. Field measurements on piled rafts with grid-form deep mixing walls on soft ground. Geotechnical Engineering Journal of the SEAG & AGSSEA, **42**(2): 1–10.

Yamashita, K., Wakai, S., and Hamada, J. 2013. Large-scale piled raft with grid-form deep mixing walls on soft ground. *In* Proceedings of the 18th International Conference on Soil Mechanics and Geotechnical Engineering (ICSMGE), 2–6 September, Paris, France, Vol. 3, pp. 2637–2640.